NATIONAL ADVISORY COMMITTEE FOR AERONAUTICS

TECHNICAL NOTE 3496

FLIGHT TESTING BY RADIO REMOTE CONTROL - FLIGHT EVALUATION OF A BEEP-CONTROL SYSTEM

By Howard L. Turner, John S. White, and
Rudolph D. Van Dyke, Jr.

Ames Aeronautical Laboratory
Moffett Field, Calif.

Washington
March 1955

1S

NATIONAL ADVISORY COMMITTEE FOR AERONAUTICS

TECHNICAL NOTE 3496

FLIGHT TESTING BY RADIO REMOTE CONTROL - FLIGHT EVALUATION OF A BEEP-CONTROL SYSTEM[1]

By Howard L. Turner, John S. White,
and Rudolph D. Van Dyke, Jr.

SUMMARY

Handling-quality flight tests were conducted with an SB2C-5 drone under radio remote control from an F6F-5 control plane. Similar tests were conducted with the drone under manual control. A comparison of these tests indicates that the beep-type, remote-control system investigated was generally satisfactory for flight testing an airplane via remote control, including take-offs and landings. The restrictions and limitations of the present remote-control equipment are discussed. Suggestions are made for modifications to improve the equipment, both for the present drone and for possible application of the remote-control equipment to high performance airplanes.

With regard to system dynamic characteristics and the corresponding autopilot parameter settings, the tests indicated that the dynamic behavior would be satisfactory if the stabilized airplane satisfied a proposed transient-response criterion.

INTRODUCTION

Remote control has been used in the past for the testing of scale models of experimental airplanes (reference 1) and for performing specialized flight tests as described, for example, in references 2 and 3 which are descriptive of the efforts of the Naval Air Experimental Station in developing a beep-type radio-remote-control system suitable for conducting structural flight testing.

The NACA has, for some time, been engaged in a broad research study directed at a detailed quantitative evaluation of the NAES remote-control system installed in a propeller-driven dive bomber. In view of the increased use of automatic control for high performance airplanes, it was

[1]Supersedes NACA RM A52A29, "Flight Testing by Radio Remote Control - Flight Evaluation of a Beep-Control System," by Howard L. Turner, John S. White, and Rudolph D. Van Dyke, Jr., 1952.

of particular interest to employ this equipment, which was available, in a preliminary study of the practical applications and limitations of servomechanism-system analysis and synthesis methods in the design of effective airplane-automatic-control combinations. Bench-test evaluations of the servo system used in this study were conducted prior to the present investigation. A correlation of predicted and measured longitudinal response characteristics of this airplane-autopilot combination are given in reference 4.

As noted previously, the NAES equipment was designed primarily for use in structural flight testing. However, it was considered desirable to examine the effectiveness of this remote-control system as a means for performing standard handling-quality flight tests in view of possible application to such flight tests under hazardous conditions. An accompanying feature of interest was the potentially greater precision and standardization in flight-test maneuvers and resultant improvement in the quality of aerodynamic data which might be obtained with automatic stabilization and maneuvering. In addition, it was believed that attempts to perform such tests requiring a wide range of precise flight maneuvers would serve to indicate many of the problems which are involved in the design of versatile automatic-control systems desired for future high-speed aircraft.

In the present investigation a comparison was made between the handling-quality flight-test data obtained by remote control and results of similar tests performed manually. The selection of the autopilot parameters, such as control gearing, control sensitivity, and rate effectiveness necessary for the satisfactory performance of a remote-controlled drone, are discussed.

The radio-remote-control equipment used in these tests was designed, built, and installed in the test airplanes at the Naval Air Experimental Station, Philadelphia, Pa. An SB2C-5 airplane (BuAer No. 83135) was equipped as a drone and an F6F-5 airplane (BuAer No. 79669) was equipped as the "mother" control plane. An auxiliary ground control station was used for landings and for take-offs. All of the remote-control tests with the SB2C-5 drone were conducted with a check pilot in the cockpit for safety reasons. The check pilot did not control the airplane during the remote-control tests.

During the course of the program, the NACA participated with the Navy in the conduct of a series of "nolo" (no live occupant in drone) structural dive tests (reference 3) of an F7F-3 drone (BuAer No. 80531) equipped with the same type of radio remote control. Brief results of these tests are presented where applicable. It is desired to express sincere appreciation to the members of the NAES test team, Project DE-205, and to the members of the staff of the Naval Air Experimental Station for

their fine cooperation in the training of NACA flight and ground personnel in the operation and maintenance of the radio-remote-control equipment.

SYMBOLS AND NOTATION

V	true airspeed, feet per second
b	wing span, feet
g	acceleration of gravity, 32.2 feet per second per second
p	rolling velocity, radians per second
δ_{A_T}	total aileron angle (sum of left and right aileron deflections, right or positive when right aileron is up), degrees
δ_E	elevator angle, degrees
δ_R	rudder angle, degrees
δ_{tab}	elevator tab angle, positive when trailing edge is down
φ	roll angle, degrees
θ	pitch angle, degrees
ψ	heading (yaw angle), degrees
c.g.	center of gravity
M.A.C.	mean aerodynamic chord

DESCRIPTION OF AIRPLANES AND EQUIPMENT

Airplanes

The SB2C-5 drone used in these tests was a single-engined, propeller-driven, two-place Navy dive bomber, a photograph of which is shown in figure 1. A detailed description of the physical characteristics of this airplane is given in appendix A of reference 5. Photographs of the check pilot's controls (front cockpit) and the parameter adjustment controls (rear cockpit) are given in figure 2. The air-to-air control plane for the drone was an F6F-5 airplane which is a

single-engined, propeller-driven, single-place Navy fighter, a photograph of which is shown in figure 3. This airplane was equipped with controls similar to those available to the drone check pilot. A photograph of the remote-control equipment in the cockpit of the F6F-5 airplane is shown in figure 4(a). A ground control station, usually situated near the downwind end of the runway, controlled the airplane during take-offs and landings. A photograph of the ground control-station console is shown in figure 4(b). The controls on the console are similar to those in the F6F-5 control plane and to the check pilot's controls in the drone.

Remote-Control Equipment

The remote-control equipment installed in the SB2C-5 drone was built around a G.E. Navy-type G-1 autopilot, utilizing electrical signals and hydraulic servo actuators. A detailed description of the autopilot is given in reference 6. Reports giving detailed descriptions of the remote-control equipment are listed in the bibliography of reference 3. A description of the control servo system installed in the SB2C-5 drone (BuAer No. 83135) is given in reference 4. The primary controls (pitch, turn, throttle, and dive controller) were operable through the autopilot, either remotely by the remote-control pilot or locally by the check pilot. The secondary controls (landing gear, landing flaps, and wheel brakes) were not connected to the remote-control system and were operated by the check pilot only at the command of the remote-control pilot. Cowl flaps were fully automatic in operation and the trim tabs were set automatically for level flight or for dives.

Pitch channel.- A block diagram of the pitch channel is shown in figure 5. Command signals to the pitch channel were either remotely initiated or initiated locally by the check pilot. Three programmed maneuvers were available to the check pilot for local operation, but only the dive controller could be operated remotely as will be discussed below. The adjustable parameters, indicated by the numbered boxes in figure 5, were: (1) autopilot trim, used to adjust the trim attitude of the drone; (2) servo follow-up sensitivity, used to adjust the autopilot control gearing; (3) control sensitivity, used to adjust the time rate of change of attitude; and (4) rate sensitivity, used to adjust the rate effectiveness. These parameters were variable in flight by the observer in the rear cockpit of the drone, but were not adjustable remotely. As can be seen from figure 5, control-gearing changes could only be made in the servo loop. Thus control-gearing changes alter not only the dynamic characteristics of the airplane-autopilot combination, but also result in changes in the dynamic characteristics of the servo system.

Dive entry, dive, and dive recovery were controlled as a programmed maneuver by the dive controller operating in the pitch channel. A block diagram of the dive controller is shown in figure 6. The dive controller consists of two intervalometers (dive and recovery), a ball-disk variable-speed drive, and a selsyn connected in series with the displacement gyro pickoff in the pitch channel. When "dive" was keyed, the disk motor and the ball carriage motor were energized and the output shaft of the ball-disk variable-speed drive rotated the selsyn. The rate of dive entry was proportional to the rate of rotation of the selsyn which, in turn, was inversely proportional to the time the dive intervalometer took to run from its preset value to zero. Mechanical stops in the selsyn limited the dive angle to some predetermined value from 0° to -120° from the horizontal (not adjustable in flight). Limit switches turned off the ball-disk drive after the dive entry and rearmed the drive mechanism for the dive recovery. The airplane remained stabilized at the given dive angle until dive recovery was keyed. The dive-entry process was then reversed with the ball-disk drive being controlled by the recovery intervalometer. Dive-recovery command signals were initiated locally by a preset altitude limit switch or by the check pilot, or remotely from the control plane. It was necessary for the check pilot to set both intervalometers locally before each dive. During the dive entry and dive recovery, while the intervalometers were operating, the signal from the rate gyro was removed from the pitch circuit.

Turn channel.- A block diagram of the turn control channel is shown in figure 7. Operation of the turn channel was much the same as for the pitch channel previously described. A turn command signal caused the ailerons and rudder to operate together, the ailerons being the primary turn control and the rudder being used only to coordinate the turn. The roll-rate and yaw-rate signals were removed from the circuit while the airplane was rolling into or out of a turn. The directional gyro was caged during the turn. The same parameter adjustments and programmed maneuver controls were available to the turn channel as were available to the pitch channel, with the exception of the dive controller.

Instrumentation

Standard NACA photographically recording instruments and a 6-channel Miller oscillograph were used to record, as functions of time, the following variables: indicated airspeed; pressure altitude; normal acceleration; roll, pitch, and yaw angles; rolling, pitching, and yawing velocities; sideslip angle; control-surface positions; and control-servo positions. No means were provided for measuring control-force data which are often of interest in a flying-qualities investigation. However, there is no reason to suppose that satisfactory control-force data could not be obtained remotely with suitable instrumentation.

Instrumentation was provided in the programmed maneuver control to introduce a step or a pulse input in each channel. The steps were adjustable in magnitude and the pulses were adjustable in magnitude and time base. These inputs were not controllable remotely but were operated by the check pilot at the direction of the remote operator.

ADJUSTMENT OF THE AUTOPILOT FOR HANDLING-QUALITY FLIGHT TESTS

In order to operate a remote-controlled drone over a wide range of airspeeds and altitudes in various flight conditions, it may be necessary to adjust the control parameters for each flight condition in order to obtain satisfactory static and dynamic airplane-autopilot characteristics over the entire flight range. To conduct the handling-qualities flight tests it was necessary to operate the drone with flap and gear down, at sea level, over an airspeed range of 85 to 120 knots for take-offs and landings; and in a clean condition, at an average altitude of 10,000 feet, over an airspeed range of 85 to 300 knots for static longitudinal stability and other flight tests.

Originally, it was planned to determine and employ optimum autopilot parameter settings at the various airspeeds over the desired test range. However, experience gained during earlier NACA investigations of this automatic control equipment indicated that a single set of adjustments might prove satisfactory over the desired test airspeed and altitude range. The tests showed that cable stretch, caused by aerodynamic loading, varied the effective gearing in a favorable manner. In the present investigation, therefore, extensive tests to determine optimum autopilot settings were limited to the clean condition at a single moderate airspeed of 130 knots. Brief tests verified the fact that the single set of adjustments so obtained was satisfactory over the desired clean-condition flight-test speed range. However, additional adjustments were necessary for satisfactory take-offs and landings to compensate for the reduced control effectiveness at low airspeeds.

Dynamic Response Characteristics

Determination of proper parameter settings.- As previously discussed, the adjustable autopilot control parameters were follow-up sensitivity, rate sensitivity, control sensitivity, and autopilot trim. Of these, follow-up sensitivity and rate sensitivity govern the dynamic characteristics of the airplane-autopilot combination. Various combinations of these sensitivities were investigated in flight, principally in the clean condition at 130 knots, to determine the proper parameter settings for use in the handling-qualities flight tests. The airplane

was flown by the check pilot who operated the remote-control equipment locally. For each parameter adjustment setting, the airplane, through the programmed maneuver control, was given a known transient disturbance in the channel being studied. Pilots' opinions of the response characteristics were obtained and the corresponding transient-response data of the airplane-autopilot combination were examined to determine which of the adjustment settings resulted in a transient response which represented the best compromise between rapid response and high damping.

Sample airplane-response time histories are shown in figures 8 and 9 for the 130 knot, clean condition. Figure 8 shows the effect of follow-up sensitivity on the longitudinal response of the airplane-autopilot combination to a step input in pitch for a constant value of rate sensitivity. The pitching response shown in figure 8(a) was considered unsatisfactory because it was too sluggish with respect both to rise time T_R (the time to rise to 90 percent of the desired steady-state value), and especially to settling time $T_{1/10}$ (the time to damp to within ± 10 percent of steady state). The pitching response shown in figure 8(b) was considered unsatisfactory because, although the rise time, T_R, was short, the response was highly oscillatory and the settling time, $T_{1/10}$, was correspondingly long. The pitching response shown in figure 8(c) was considered the optimum obtainable compromise between short settling and rise times and corresponds to the parameter adjustments used for the flight tests.

The transient-response characteristics in roll and yaw corresponding to the optimum parameter settings used in this investigation are shown in figure 9. The follow-up sensitivity and rate sensitivity settings determined from these tests and used in the handling-quality flight tests are shown in table I. The lateral results presented in table I and in figure 9 were obtained from tests of the rudder and aileron channels individually while the other control was locked. However, tests in the more general condition of simultaneous rudder and aileron channel operation indicate that the optimum settings were practically the same in either condition. It should be noted in figure 9 that a pulse transient was used in the rudder channel because the airplane-autopilot combination was spirally divergent to a step rudder input with ailerons locked.

Parameter settings required for satisfactory take-off and landing characteristics which, as will be discussed later, differ from the optimum clean-condition settings, are also shown in table I.

Comparison of results with proposed specifications.- Proposed specifications for response characteristics of airplane-autopilot combinations considered acceptable for use in structural flight testing are given in reference 7. Sufficient data were obtained during the course of the NACA evaluation of the airplane-autopilot combination employed in the present tests to permit a detailed comparison of the results with that portion of the specification of reference 7 which deals with the dynamic characteristics in pitch. Under "Flying Qualities Required of Remotely Controlled Aircraft for Structural Flight Tests," paragraph 1(a) of reference 7 reads:

> "Longitudinal motion - Oscillations in pitch due to a step pitch disturbance shall damp to within 10 percent of steady state within 2 seconds and within one cycle....."

It appears that this single specification seeks to guarantee a desirable combination of rapid response and good damping by limiting to 2 seconds the time required to reach and never again depart more than ±10 percent from the desired new steady-state value. The limit of one cycle serves to guard against a poorly damped, short-period oscillation.

Values of time to damp to within 10 percent of steady state and cycles to damp to within 10 percent of steady state for the airplane-autopilot combination have been evaluated for various combinations of follow-up and rate sensitivities from data such as given in figure 8. These results are shown in figure 10 as a function of follow-up sensitivity settings for various constant values of rate sensitivity at 130 knots and at 10,000 feet. The boundary specified in reference 7 is shown for comparison. The fact that the combination of settings considered optimum in the present test plots at the greatest possible distance from the boundary is an indication of the validity of the requirement. Examination of recorded transients and pilots' opinions showed that combinations of follow-up and rate sensitivities which gave dynamic characteristics falling on the satisfactory side of the boundary would be acceptable for the handling-quality tests, whereas those falling on the unsatisfactory side would be unacceptable for such tests (for example, see "Dives" in text).

Reference 7 offers the following requirements on lateral motion similar to that discussed above for the longitudinal motion:

> "Lateral Motion - Oscillations in roll and yaw due to step roll or yaw disturbances shall damp to within 10 percent of steady state within 4 seconds and within two cycles."

Although insufficient data were available to permit detailed comparison for the roll and yaw cases, the results of the present tests indicate that, as in the longitudinal case, the lateral motion requirement of

reference 7 is at least qualitatively a useful one. The roll response for the optimum aileron parameter settings, as shown in figure 9(a), easily satisfy the requirement. Since it was necessary to use a pulse rather than a step input in the rudder channel, the optimum test response shown in figure 9(b) cannot be compared directly with the requirement; however, neglecting the divergent airplane-motion characteristic of the system with the ailerons locked, it appears that the yawing response meets the intent of the requirement.

Static Control Characteristics

Of the adjustable control parameters, control sensitivity and autopilot trim may be considered as the static parameters which regulate the static control characteristics of the stabilized airplane. Control sensitivity (box 3, figs. 5 and 7) regulates the excitation of the selsyns driven by the pitch or the turn motor and hence governs the time rate of change of attitude. This parameter is effective only when the command signal is initiated from a source other than the programmed maneuver control and then only effects the magnitude of the response characteristic. In the optimization of the dynamic response characteristics previously discussed, control sensitivity thus has no effect. Autopilot trim or bias is a static control parameter used to adjust the trim attitude of the drone for any particular flight condition. The optimum control sensitivity and autopilot trim settings were determined by the check pilot operating the remote-control equipment from the cockpit of the SB2C-5 drone. The values of control sensitivity for flight testing, take-offs, and landings are given in table I.

TESTS, RESULTS, AND DISCUSSION

As discussed previously, the NAES remote-control gear installed in the SB2C-5 airplane was designed primarily for structural flight testing. Although the maneuvers provided by the equipment for such structural tests are useful in standard flying qualities or associated aerodynamic research investigations, additional maneuvers, particularly lateral and directional, are necessary in complete flying-qualities evaluations. In the present investigation an attempt was made to perform important flying-quality maneuvers which could be obtained through reasonable modifications to the basic gear and to flight techniques. The maneuvers and data desired in a flying-qualities evaluation can be deduced from the Navy and Air Force specifications for handling qualities of piloted airplanes (references 8 and 9). The maneuvers may be divided roughly into three phases: longitudinal, lateral-directional, and stalls. The remote-control equipment used in this investigation was not suitable for use

near the stall. In the following discussion, the tests have been divided into longitudinal and lateral-directional phases according to the predominant characteristic of the data obtained in each type of test.

Longitudinal Phase

Static longitudinal stability.- For evaluating static longitudinal stability, the airplane is trimmed to fly at a given angle of attack in steady, straight, wings-level, unaccelerated flight at a given power setting; changes in airspeed are then made by changing pitch attitude and the variation with airspeed of the elevator angle required for trim is used as a measure of the static longitudinal stability of the stabilized airplane.

No alterations to the remote-control system were required to perform these tests. The throttle of the drone was adjusted remotely from the F6F-5 control plane to give level flight at 180 knots at 10,000 feet, corresponding to normal rated power, and the throttle setting remained fixed throughout the tests. The control plane was flown at various airspeeds over the desired range and attitude command signals were transmitted to the drone which resulted in steady flight at the same airspeed as that of the control plane. The lateral-directional stabilization system maintained the drone in straight, wings-level flight. For comparison, the tests were repeated with the SB2C-5 under the manual control of the check pilot. The data obtained under both remote and manual control are presented in figure 11, in which sideslip, rudder, and elevator angles required for steady, wings-level, unaccelerated flight are plotted as a function of indicated airspeed. It is seen that the data obtained by remote operation are of good quality and are in excellent agreement with the data obtained in manual flight.

Dives.- With regard to longitudinal flying qualities, dives and dive pull-outs are of interest principally in establishing high-speed static and maneuvering stability characteristics. Satisfactory steady-flight data were obtained in dives up to the highest test speed of 302 knots and satisfactory dive attitude stabilization has been obtained in NAES tests at dive angles up to -110°. For the evaluation of longitudinal maneuvering characteristics, data (principally elevator angle) obtained at the same airspeed and altitude during turns or pull-outs of different steady normal accelerations are desired. Gyro limitations under remote control restricted the bank angles and hence the acceleration factors that could be obtained in steady turning flight. Therefore, in the present program, a series of dives were entered from level flight at about 120 knots at 11,000 feet; pull-outs which would yield the desired steady maneuvering data were then initiated at about 200 knots.

The entry, dive, and recovery were controlled from the F6F-5 control plane, except that the drone check pilot was required to reset the dive and recovery intervalometers locally for each dive.

As previously noted, the pitch-rate feedback was removed from the circuit during dive entry and recovery involving the automatic dive controller. It was found, as indicated in figure 10, that the transient response with zero rate sensitivity and the generally optimum follow-up sensitivity setting of 40 was highly oscillatory. A follow-up sensitivity setting of 55 was used in the dive program to give the greatest damping available under this zero rate feedback condition. A sample time history of an automatic controlled dive under these conditions is presented in figure 12(a). It should be noted in figure 12(a) that the parameter settings of rate sensitivity 30, follow-up sensitivity 55, resulted in a mildly oscillatory flight condition which was considered marginal by the check pilots. This combination of parameter settings represents a boundary condition as shown in figure 10(b). It is also seen in figure 12(a) that the normal acceleration during the dive recovery was still oscillatory and it was difficult to ascertain steady maneuvering characteristics from such dive recoveries. A smoother dive recovery obtained manually is illustrated in figure 12(b). Tests therefore were made to determine the effects of follow-up sensitivity and the rates of entry and recovery on the pitching oscillation during the dive entry and the dive recovery. The effect of follow-up sensitivity setting on the recovery acceleration time history at constant values of recovery airspeed, dive angle, dive recovery setting (recovery intervalometer), and rate sensitivity is shown in figure 13(a), and is seen to be too small to be of practical significance. The effect of dive-recovery setting (recovery intervalometer) on the recovery acceleration time histories is shown in figure 13(b). It is seen that although the acceleration response was oscillatory, a reasonably long period of approximately constant acceleration could be obtained by increasing the time interval over which the intervalometer operates (low intervalometer settings). Use of low intervalometer settings unfortunately limited the value of normal acceleration which could be obtained. However, low intervalometer settings in conjunction with a high follow-up sensitivity setting appeared to offer the best compromise for the present tests. Accordingly, a series of dives with recoveries of various severity were performed at about 180 knots. The measured variation of normal acceleration factor, pitching velocity, and elevator angle are given in figure 14 as a function of lift coefficient, C_L. Data taken in similar pull-outs performed manually are shown for comparison. The variation of trim elevator angle with lift coefficient for the remote-control procedure was smooth and similar in shape to that for the manual procedure. The sizable difference in level between the two curves, corresponding to a change in straight-flight trim elevator angle of about 2.7°, could not be accounted for completely, although some of the discrepancy is due to differences in center-of-gravity location and trim-tab setting.

The remote-control equipment used in this investigation was designed primarily for performing structural dive tests, one important phase of which involves pull-outs at speeds and accelerations greater than those reached in the present tests. Control characteristics in these more severe maneuvers are also important flying qualities. Thus, the results of such tests with similar gear installed in an F7F-3 drone airplane are of interest. The F7F-3 drone was flown nolo by the Navy in conjunction with the NAES in a series of three dives and recoveries intended to explore the upper limits of the velocity-acceleration diagram. Each dive recovery was initiated automatically at a predetermined altitude by a pressure switch located in the drone. The dive angle was fixed at -30° from the horizontal and the rate of recovery was fixed at 10.7° per second. Different recovery accelerations were obtained by varying the dive entry altitude such that the drone would attain a given predicted airspeed when the preset recovery altitude was reached. Results of these dive tests are shown in figure 15. Correlation between the predicted and actual results was considered satisfactory, although the test conditions were generally more severe than had been intended. It should be noted that the last test point is low, probably because the aerodynamic forces on the elevator were of such magnitude as to cause a reduced recovery rate as a result of insufficient servo power.

As was the case in the present SB2C-5 tests (figs. 12 and 13) the normal accelerations during the dive entry and recovery were undesirably oscillatory due primarily to lack of a pitch rate or equivalent damping signals. It appears that this difficulty might best be overcome by use of some dive command and stabilization system other than the present one, which is essentially an "attitude only" system during an automatic dive entry or recovery. One possibility is the acceleration command-type system which has been given preliminary study by NAES in reference 10. Incorporation of an airspeed sensing switch to initiate the dive recovery might also be desirable in order to permit greater flexibility and accuracy in producing a pull-out at a desired airspeed; note the differences between the desired (or predicted) and the actual airspeeds in figure 15 when altitude-sensing dive-recovery initiation was used.

Take-offs.- For take-offs, the rudder must provide sufficient control to maintain straight paths on the ground during take-off runs, and the elevator must provide adequate control at low airspeeds to maintain any attitude up to the level position. (See references 8 and 9.) Although tests were not made to determine the take-off characteristics of the drone under the specific conditions required by references 8 and 9, take-offs made under normal operating conditions for the remote-controlled drone adequately demonstrated the feasibility of performing such tests under remote control. For the remote controlled take-offs, the parameter settings normally used for flight must be altered to compensate for the reduced control effectiveness at low airspeeds. Although most of the control parameters of each channel were changed,

the greatest changes were made in the rudder channel parameters since directional control during the take-off run is accomplished by use of the rudder. The parameter settings resulting in the best take-off characteristics are given in table I.

Take-offs were controlled from a ground control station located alongside the runway, near the starting point for the take-off run. The drone was taxied into position and alined with the runway by the check pilot. When ready for take-off, the check pilot released the brakes and transferred control to the ground control station. The ground control pilot applied power gradually and controlled the elevator to effect a take-off. Directional control was maintained automatically by the directional and directional-rate gyros through the rudder and was excellent for these propeller-driven airplanes. However, if the ground control pilot attempted to key a turn during take-off, the special parameter settings for take-off would be replaced with the normal flight settings and the rate and directional gyros would be removed from the circuit momentarily. The first reaction to a keyed "turn" would be the centering of the rudder, followed by a marked reduction in directional control at low airspeeds.

Time histories of remote-controlled and manually-controlled take-offs are shown in figure 16. Figure 16(a) is a time history of a ground-controlled take-off of the SB2C-5 drone under a slight cross wind. Figure 16(b) is a time history of a ground-controlled, nolo take-off of an F7F-3 drone under a cross-wind condition of 35 knots from 30° left of the runway center line. Figure 16(c) is a time history of a manual take-off of the SB2C-5 drone with no cross wind. The extreme control-surface oscillations shown in figure 16(a) are caused by inherent characteristics of the gyros and are of such a frequency and occur at such low airspeeds as to have no appreciable effect on the airplane during the take-off run. Control of the propeller-driven drones in the take-offs shown in figures 16(a) and (b) was highly satisfactory. Examination of the time histories in figures 16(a) and 16(c) shows that there is less rolling motion after take-off and less heading change during take-off than experienced under manual control. It should be noted that relatively little training was required for an experienced test pilot to become proficient in controlling a take-off from the ground control station.

Landings.- For landings, the ailerons and rudder must provide sufficient control to maintain straight, wings-level flight at low landing approach airspeeds, and the rudder must provide sufficient control to maintain straight landing ground paths. The elevator must provide sufficient control to permit smooth touchdowns over a range of low airspeeds approaching the stall. (See references 8 and 9.) As in take-offs, tests were not made to determine the landing characteristics under the exact conditions specified in references 8 and 9, but these were

studied under the normal operating conditions for the remote-controlled drone. Again, the parameter settings differ from the normal flight settings to compensate for the reduced control effectiveness at low airspeeds. As shown in table I, the parameter settings resulting in the best landing characteristics are similar to those used for take-offs excepting that large rudder-rate sensitivities are not required for landings. The parameter settings generally give larger and more rapid surface motions for a given signal than are necessary for normal flight.

Drone landings were remotely controlled from a ground control station located some 50 feet to one side of the runway and approximately opposite the point where the initial touchdown was to be made. The drone, under the command of the control plane, was alined with the runway with its flaps and gear down and at a throttle setting that was held fixed until the final cut. Control was turned over to the ground control station when the drone was approximately 2 miles off the end of the runway. The drone airspeed was controlled by changing its attitude. When the drone was over the runway in the proper position for landing the power was cut and a landing accomplished. A wave-off could be controlled by the ground control station if conditions warranted such action. For landing runs after touchdown, brakes were controlled by the check pilot in the SB2C-5 drone, and remotely by the ground station for the F7F-3 drone.

Considerably more training was required for an experienced test pilot to become proficient at controlling the drone in landings than was required for take-offs. Maintenance of precision directional control, sufficient to effect a landing on a runway, was most critical, particularly when landings were made under cross-wind conditions. Thirty-six landings were made during the training period. Of the first nine landings, four touchdowns were accomplished, none of which were particularly satisfactory; two wave-offs were made under remote control; and the check pilot took over control three times prior to touching down. On the last series of nine landings, the check pilot took over control prior to touchdown only once. Of the other eight landings in this series, five were excellent and three were not satisfactory, although loss of the drone in remote operation would probably not have occurred. Of the entire 36 training landings, 22 touchdowns and 14 wave-offs were made. Of the 22 touchdowns only 5, made under adverse cross-wind conditions, were poor enough to have possibly caused damage to a nolo drone.

Time histories of remote-controlled landings are shown in figures 17(a) and (b). A time history of a manually controlled landing is shown in figure 17(c). Figure 17(b) indicates that control was satisfactory for remote-controlled landings even under 35-knot, 30° cross-wind conditions, although directional control after touchdown was difficult

in a cross-wind condition due to the weathercocked attitude of the airplane at the touchdown.

Directional control on the ground was accomplished by brakes and by turn control. "Turn" could be keyed during a landing run when there was sufficient airspeed for control effectiveness. Keying "turn" caged the directional gyro which was uncaged after the turn was completed, allowing the airplane to hold the new heading. Keying "brakes" transferred the rudder-channel signal to the brake channel, resulting in equalized braking action. When "brakes" and "turn" were keyed simultaneously, differential braking pressure was applied so as to turn the airplane in the direction indicated by the turn signal. However, because of circuit design, the directional gyro was not caged in this case and when the turn signal was removed with "brakes" still being keyed, the error signal from the directional gyro caused the airplane to resume the original heading. Hence, remote directional control with the brakes and turn was difficult because the airplane tended to follow an erratic course. Because of the operational difficulties with the braking system, the brakes on the SB2C-5 drone were disconnected from the remote-control system and were operated manually by the check pilot. Another braking difficulty lay in the application of full braking power when "brakes" were keyed. This arrangement could be improved by operating the brakes in the same manner as the throttle, wherein any increment of braking power could be applied; however, the differential braking features should be retained.

Changes in direction under remote control were accompanied by changes in roll angle, hence larger angles of roll were developed during the final approach under remote control than under manual control. This feature made it difficult to make corrections in direction when the drone was close to the ground just prior to the touchdown. This system might be improved by transferring directional control during the final landing approach to the rudder only, leaving the roll stabilization, through the ailerons, to maintain a wings-level attitude. In general, the final approaches were flatter under remote control than under manual operation; however, actual touchdown speeds were not widely different.

Longitudinal dynamic stability.- Tests were conducted under manual control and under remote control to determine the longitudinal dynamic stability characteristics of the test airplane. Under remote control, with the airplane destabilized in pitch, an elevator pulse input was introduced with the pulse generator. Gyro stabilization in pitch was removed by disconnecting the output signals of the pitch-rate and pitch-displacement gyros while the drone was being flown at the desired airspeed in a trimmed, wings-level attitude. Although the drone was under the control of the pilot in the control plane, destabilization in pitch and initiation of the pulse input were locally controlled at the direction of the remote pilot.

Time histories of a remote-controlled and a manually-controlled pitch oscillation are shown in figure 18. Although the magnitude of the remote induced pulse is smaller and the pulse time base larger than for the manual pulse input, the free oscillation resulting from the mechanical inputs is similar to that from the manual input. Since the airplane was almost critically damped, due to low static stability, no well-defined longitudinal oscillations resulted from these maneuvers over the permissible speed range.

Lateral Phase

Turn control.- As was previously noted, the remote-control equipment used in these tests was set up for maximum bank angles of 30° and hence the gear was not suitable for evaluating longitudinal maneuvering characteristics in turns. However, performance of the turn control within this limited range is of interest in connection with the flying-qualities tests where the control manipulations required to enter and maintain a steady coordinated turn are of some importance. Time histories of abruptly entered, 30°-banked, steady turns under remote and manual control are shown in figure 19. The angle-of-bank records show that the turn entry was slightly more rapid and that the angle of bank was held more precisely under remote control. However, it was necessary for the remote pilot to beep up-elevator to prevent excessive altitude loss during the turn.

The sideslip records show deficient coordination under remote control; about 3° sideslip is indicated in figure 19(a). This lack of coordination is inherent in the automatic-turn-control system wherein the rudder angle applied is directly proportional to the bank angle irrespective of the aerodynamic forces acting on the airplane. Thus it would be expected that turn coordination could be attained at only one airspeed, bank angle, and turn direction for any given set of parameter adjustments. This was verified during the present flight tests.

For flying-qualities evaluations and for other automatic control applications, provision should be made for perfect automatic turn coordination up to 90° bank over the allowable operating speed range. Sideslip or lateral acceleration signals might be used to attain the desired turn coordination.

Sideslips.- In flying-qualities evaluations the variation of rudder angle, aileron angle, and angle of bank with sideslip angle, as obtained in steady-straight sideslips, are indicative of the directional static stability, dihedral effect, and cross-wind force characteristics. Major alterations to the present remote-control equipment would be required to perform steady-straight sideslips in which the cross-wind forces due to

sideslip are balanced by banking the airplane in the direction of slip. However, it was possible to perform wings-level flat turns in which the side force due to sideslip caused the turn. With regard to the rudder and aileron angles required for balance, the maneuver was similar to a steady-straight sideslip except for the usually negligible aerodynamic influences of yawing velocity.

The flat turns were performed by remotely keying "turn" after the yaw gyro stabilization had been locally removed and the aileron-control sensitivity (see fig. 7) had been reduced to zero. The roll gyro stabilization maintained the drone in a wings-level attitude and keying "turn" moved the rudder to produce the sideslipped attitude and the resulting flat turn. A comparison of the sideslip data obtained under remote control with similar data obtained by manual control in steady straight sideslips is given in figure 20. Good correlation was obtained for control angles over the range of sideslip angles investigated, which indicated that the yawing velocity effects were negligible. In fact, the yawing velocities were too small to be measured accurately with available instrumentation, and no quantitative evaluations of the side-force characteristics could be made.

Aileron rolls, rudder fixed.- In a handling-qualities evaluation, one indication of the ability of the ailerons to provide satisfactory roll control is the maximum helix angle, $pb/2V$, that the wing tip describes in space following an abrupt, rudder-fixed, step deflection of the ailerons. Such maneuvers were by far the most difficult to perform with the remote-control system being investigated. It was necessary to remove the gyro stabilization from the roll, pitch, and yaw axes of the drone, thereby requiring the remote-control pilot in the control plane to use visual references in stabilizing the drone. It was necessary to remove the pitch gyro stabilization because of the interaction of the pitch rate gyro due to yawing during the rolling, and because of the interaction of the pitch displacement gyro due to lateral accelerations. The yaw channel was destabilized so that the rudder would remain fixed. Since the recording gyro was limited to $\pm 70^{\circ}$, and the required rates of roll could not be established in 70° of bank, it was necessary to start the maneuver with the drone in a steady banked attitude of as much as 35°. The 30° limitation in bank angle imposed by the stabilization system was eliminated by destabilizing in roll. The drone was then rolled to the opposite side using a step aileron deflection as a programmed maneuver. When the airplane approached the limits of the recording roll gyro, a step of opposite magnitude was keyed which returned the airplane to its original position. It would be possible to perform a maneuver of this type by programming so that the remote pilot would just key an aileron roll; but under the present system, the programming of the maneuver was controlled by a step generator whose signal was initiated locally at the instructions of the remote pilot in the control plane. A comparison of the aileron-roll data obtained remotely

with data obtained manually using normal flight-test techniques is given in figure 21. Good correlation was obtained over the range of aileron deflections investigated. The difficulties in performing these maneuvers remotely could have been greatly reduced if gyros with 360° freedom in roll were used.

Dynamic lateral stability.- No particular difficulties were encountered in performing the dynamic lateral-stability tests under remote control. The yaw gyro stabilization was removed and the drone was placed in a sideslipped attitude in the same manner as described previously under sideslips. The lateral oscillations were induced locally by removing both the turn signal and roll stabilization, a procedure which centered and held fixed both ailerons and rudder. Time histories of lateral oscillations initiated from a sideslip under remote control and under manual control are given in figure 22. The rudder motions shown in figure 22 are the result of structural flexibility and cable stretch in the rudder-control system. A comparison of the lateral period and damping over the speed range under both methods of control is shown in figure 23. Correlation was excellent over the speed range investigated.

CONCLUDING REMARKS

The NAES beep-type remote-control equipment installed in the test SB2C-5 drone was designed primarily for structural flight testing. Although some of the maneuvers used in structural flight testing are similar to those used in a flying-qualities investigation, the equipment could not be expected to be completely satisfactory in the performance of the numerous and diverse maneuvers required in a flying-qualities evaluation. However, with regard to maneuvers and required equipment performance common to both types of remote-control testing (and most other applications of remote control to aircraft), the equipment generally was satisfactory for use in the SB2C-5 drone. The radio-remote-control equipment was satisfactory for control of take-offs and landings in cross winds up to at least 35 knots at 30°. Take-off control was excellent, especially in view of the high torque effect of the propeller-driven test airplanes, and a relatively small amount of training was required for ground-operator proficiency. Landings, especially under cross-wind conditions, produced control difficulties after touchdown and considerably more training was required for ground-control-pilot proficiency than was required for take-offs. In other phases of flight, control of the drone from the airborne control stations was satisfactory and did not require extensive training for experienced test pilots to become proficient remote-control pilots.

In some cases it was necessary to improvise and rearrange the existing control system considerably to perform various flying-qualities maneuvers such as aileron rolls and sideslips. In some cases it was not possible to perform the desired maneuvers because of fundamental limitations of the system. For example, turning maneuvers were restricted to 30° bank because of roll-gyro limitations. The provision for automatic control coordination in turns was inadequate, and the automatic dive controller did not yield the desired steady acceleration maneuvers.

In addition to the difficulties mentioned above, the present flying-qualities program and previous NACA investigations of this NAES equipment indicated a number of characteristics which, although not seriously deficient for the SB2C-5 drone, probably would have to be improved if application to high performance airplanes were considered for either flying-qualities tests or for any other operations requiring wide flexibility in maneuvering and operating conditions. For example, the power of the hydraulic servos would be insufficient for many high-speed airplane applications. Means of varying control gearing without varying servo dynamic characteristics would be necessary in order to obtain optimum over-all system characteristics. Some form of automatic gain changer would also be required to obtain optimum, or even satisfactory, behavior over a wide range of flight altitudes and airspeeds.

With regard to system dynamic characteristics and the corresponding autopilot parameter settings, the test program indicated that the dynamic behavior would be satisfactory if the stabilized airplane satisfied transient response and damping criterion proposed by NAES. In the present investigation proper autopilot parameter settings were determined from preliminary flight tests with a check pilot in the drone. However, it appears that proper settings could be determined analytically, prior to the first flight, from suitable airplane response data and autopilot bench-test results.

Ames Aeronautical Laboratory
National Advisory Committee for Aeronautics
Moffett Field, Calif., Jan. 29, 1952

REFERENCES

1. Stout, Ernest G.: Development of Precision Radio-Controlled Dynamically Similar Flying Models. Jour. Aero. Sci., vol. 13, no. 7, July 1946, pp. 335-345.

2. Arnold, J. B.: Development of Remote Control Flight Test Techniques; F6F-5K Nolo Flight Test Program. Naval Air Experimental Station, Phila., ASL NAM 2431, pt. V, Aug. 1950.

3. Arnold, J. B.: Service Testing of NAES Remote Control Equipment; F7F-3 Nolo Flight Test Program. Naval Air Experimental Station, Phila., ASL NAM DE-205.1, pt. I, May 9, 1951.

4. Smaus, Louis H., Gore, Marvin R., and Waugh, Merle G.: A Comparison of Predicted and Experimentally Determined Longitudinal Dynamic Response Characteristics of a Stabilized Airplane. NACA TN 2578, 1951.

5. Turner, Howard L.: Measurement of the Moments of Inertia of an Airplane by a Simplified Method. NACA TN 2201, 1950.

6. Anon.: Operation and Service Instructions for Automatic Pilot, Type G-1, GE Model 2CJ1A1, General Electric. (AN 05-45AE-1), revised Aug. 1946.

7. Rogin, L., and Gottlieb, S.: Specifications for Response Characteristics of Autopilot Servomechanisms Required to Stabilize High Speed Aircraft for Structural Flight Tests. Naval Air Experimental Station, Phila., ASL NAM 2432, pt. IV, Nov. 15, 1949.

8. Anon.: Specification for Flying Qualities of Piloted Airplanes, Bur. Aer. Specification, NAVAER SR-119B, June 1, 1948.

9. Anon.: Flying Qualities of Piloted Airplanes. U. S. Air Force Specification No. 1815-B, June 1, 1948.

10. Rogin, L., and Visconti, L.: Load Factor as a Means of Autopilot Error Control for Longitudinal Stabilization of High Speed Aircraft in Structural Flight Test Maneuvers. Naval Air Experimental Station, Phila., ASL NAM 2432, pt. V, May 2, 1950.

TABLE I.- OPTIMUM CONTROL-PARAMETER SETTINGS

Parameter	Channel	Units	Flight condition					
			Flight		Take-off		Landing	
			Dial setting	Value	Dial setting	Value	Dial setting	Value
Displacement gyro constant	Rudder	volts/$^{o}_{\psi}$	--	0.50	--	0.50	--	0.50
	Aileron	volts/$^{o}_{\varphi}$	--	.56	--	.56	--	.56
	Elevator	volts/$^{o}_{\theta}$	--	.51	--	.51	--	.51
Servo follow-up sensitivity	Rudder	volts/$^{o}_{\delta_R}$	50	.38	35	.25	45	.33
	Aileron	volts/$^{o}_{\delta_{A_T}}$	45	.40	45	.40	45	.40
	Elevator	volts/$^{o}_{\delta_E}$	40	.31	30	.23	30	.23
Rate sensitivity	Rudder	volts/$\dot{\psi}$	40	22	75	40	40	22
	Aileron	volts/$\dot{\varphi}$	30	14	45	22	45	22
	Elevator	volts/$\dot{\theta}$	30	16	30	16	30	16
Control sensitivity[1]	Rudder	[2]$^{o}_{\delta_R}/^{o}_{\varphi}$	10	.17	30	.61	30	.61
	Aileron	$^{o}_{\varphi}$/sec	100	10	100	10	100	10
	Elevator	$^{o}_{\theta}$/sec	40	2.3	60	3.4	60	3.4

[1]Selected for best performance by the check pilot operating the remote-control equipment from the cockpit of the SB2C-5 drone.

[2]In turns, the ailerons are the primary turn control; the rudder is used only to coordinate the turn. The rudder angle is proportional to the angle of bank.

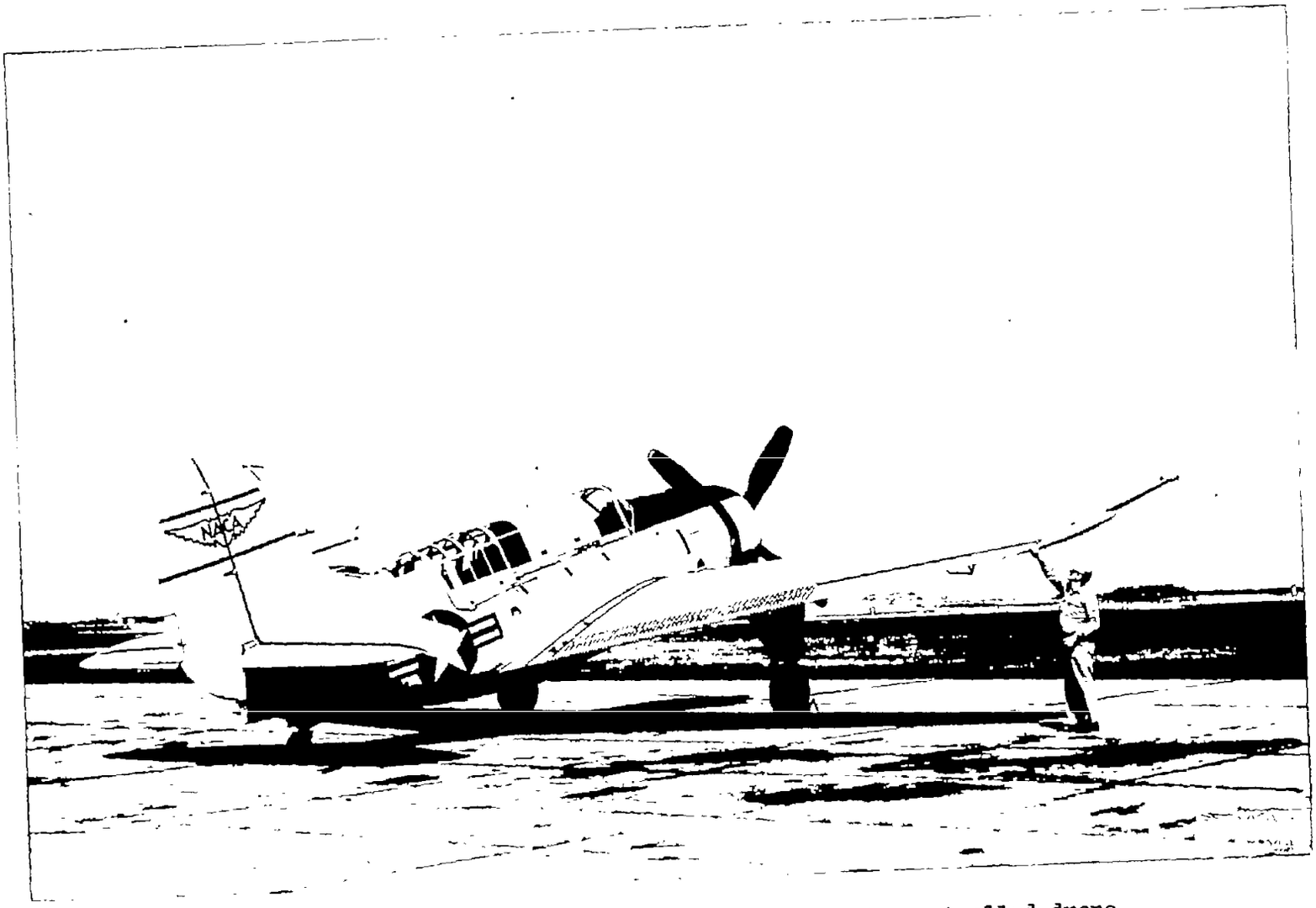

Figure 1.- Three-quarter rear view of SB2C-5 remote-controlled drone.

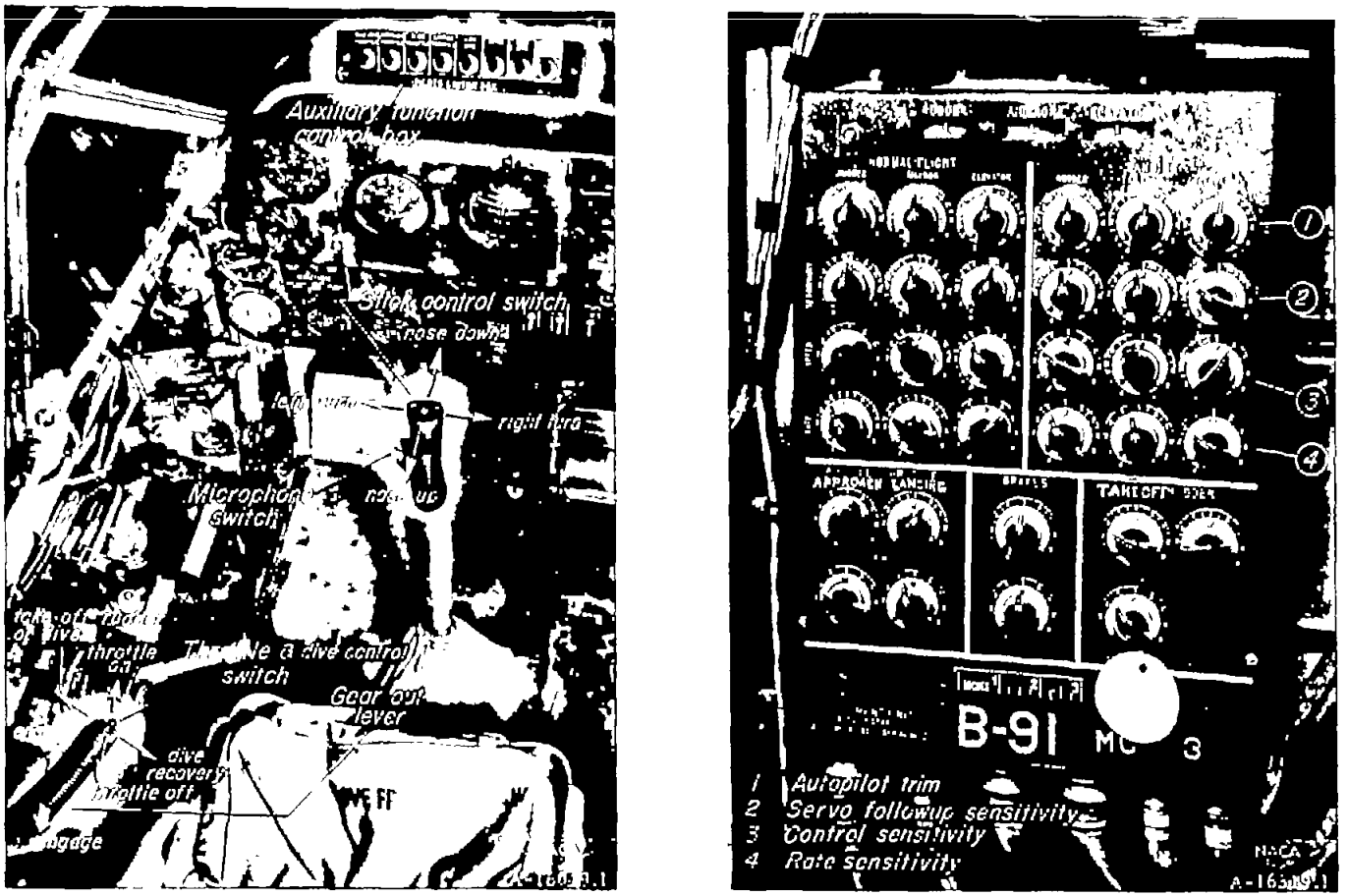

(a) Front cockpit.

(b) Rear cockpit.

Figure 2.- Check pilot's controls and parameter adjustment controls in SB2C-5 drone.

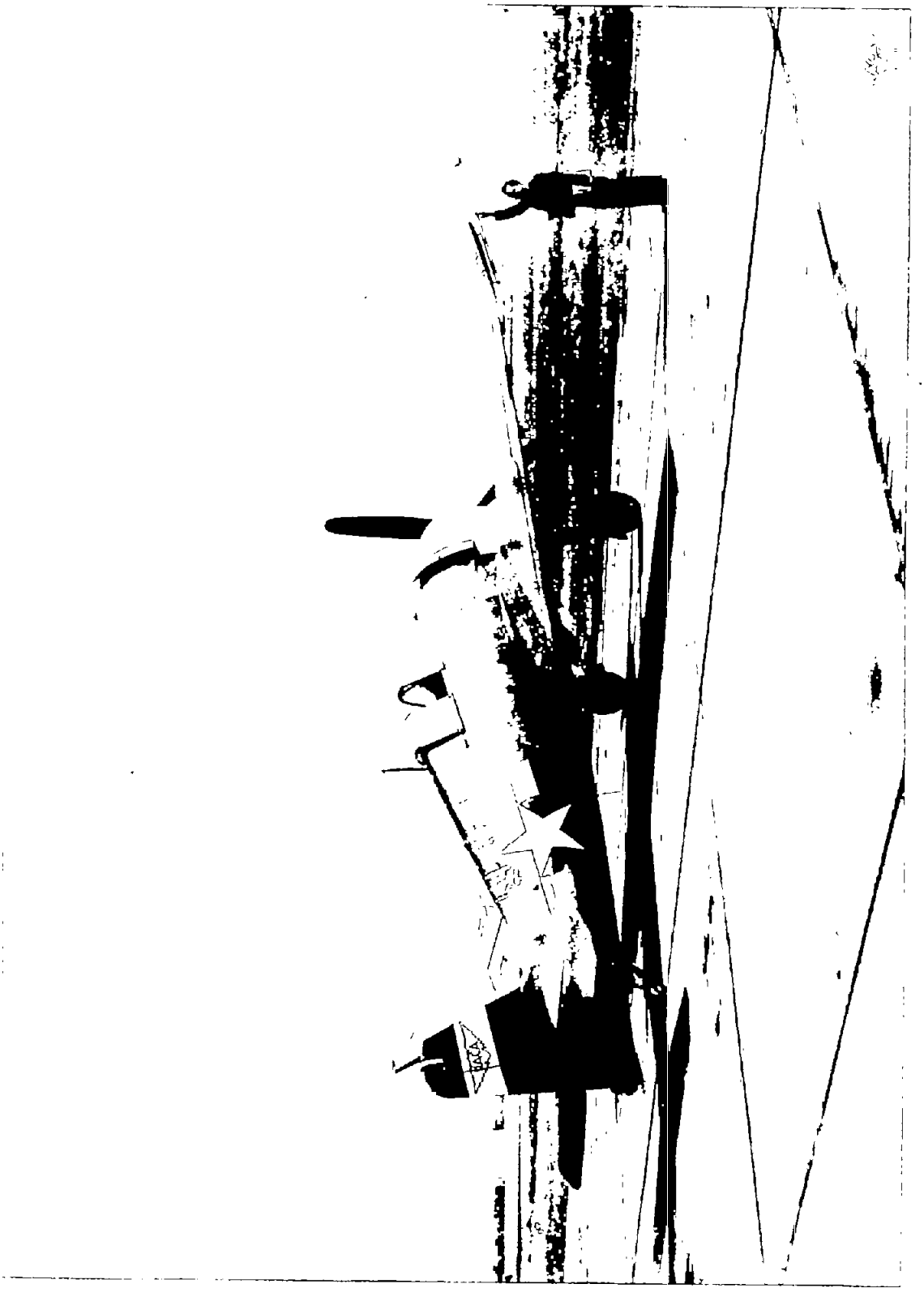

Figure 3.- Three-quarter rear view of F6F-5 air-to-air control plane.

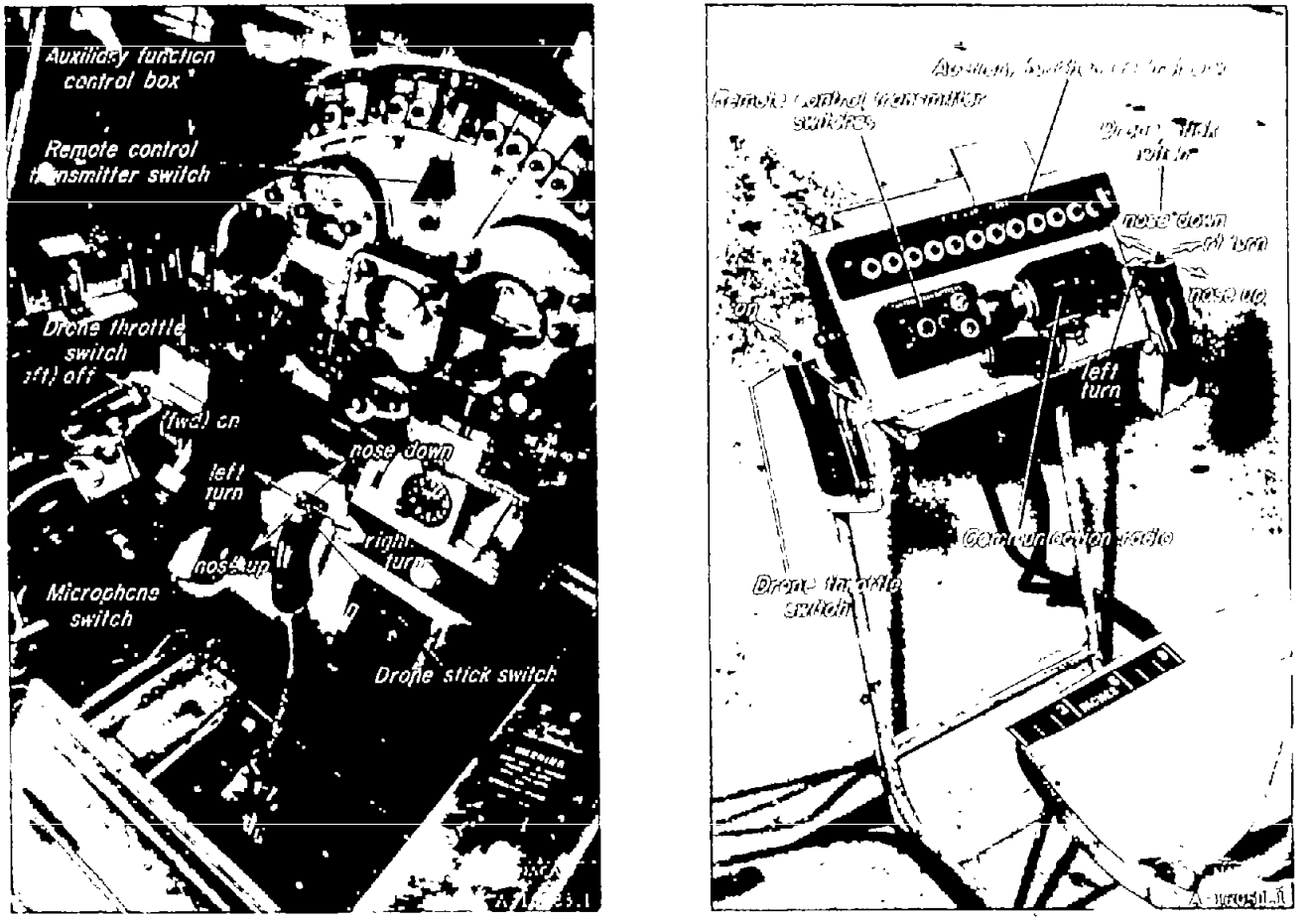

(a) Cockpit F6F-5 control plane.

(b) Ground control station console.

Figure 4.- Controls for remotely controlling SB2C-5 drone.

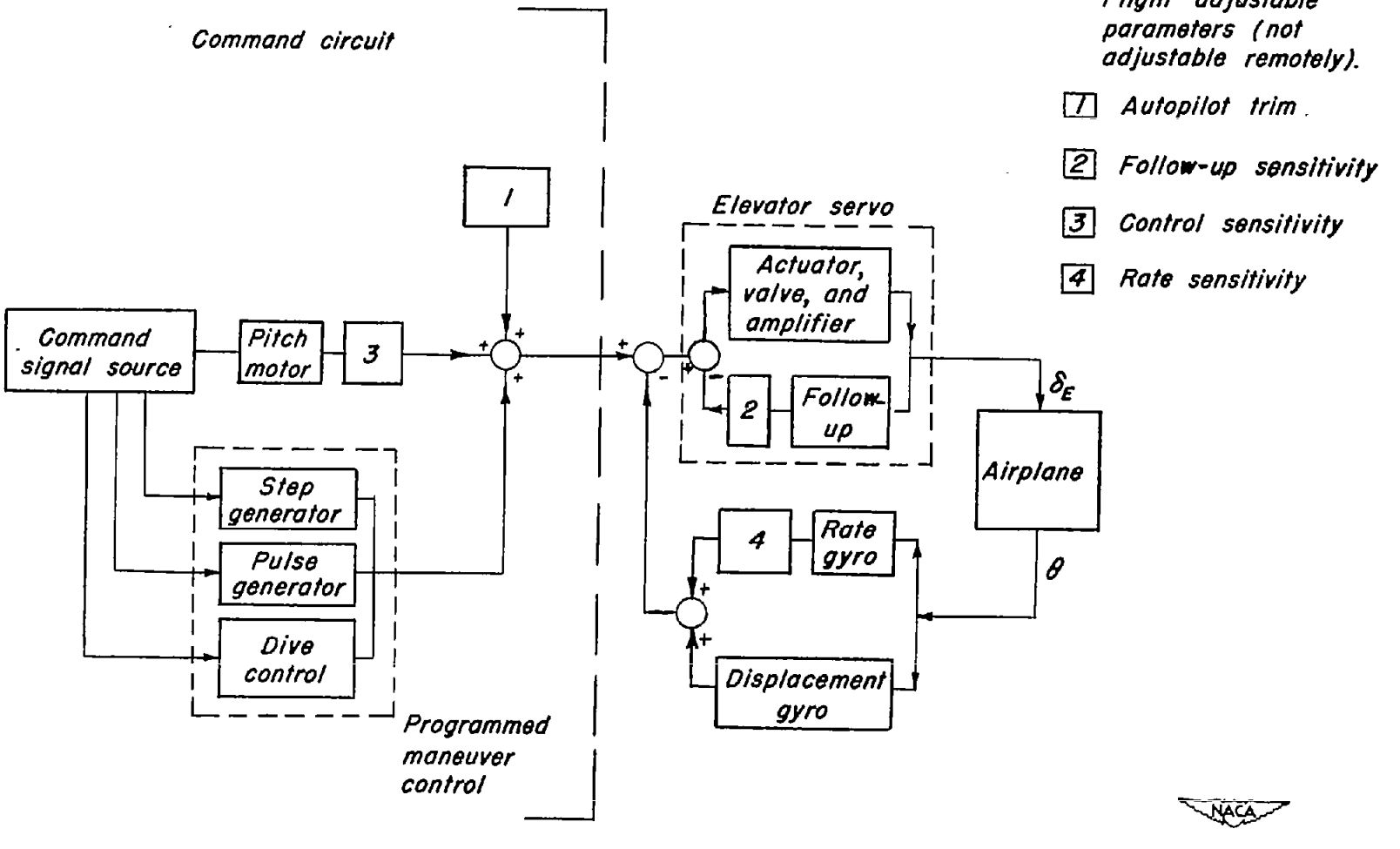

Figure 5.- Block diagram of pitch channel, remote-controlled SB2C-5 drone #83135.

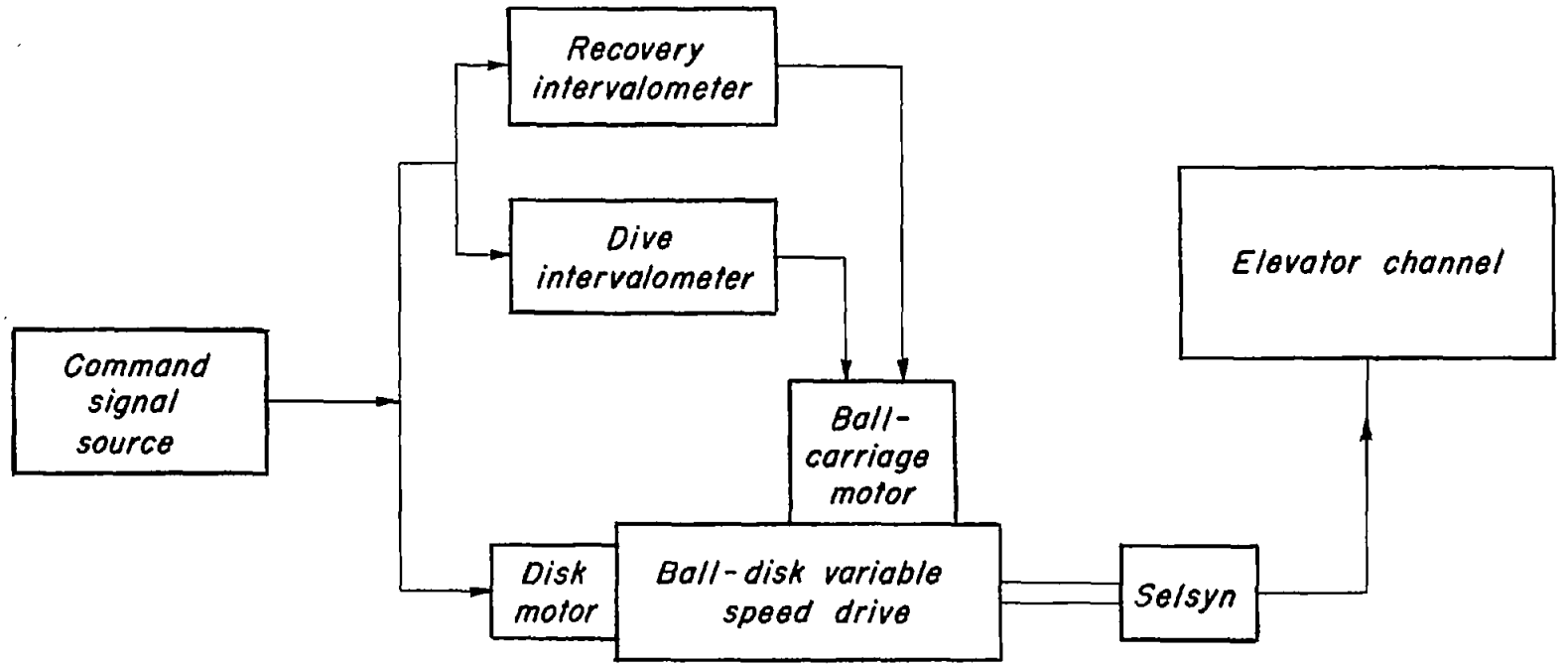

Figure 6.- Schematic diagram of dive controller, remote-controlled SB2C-5 drone #83135.

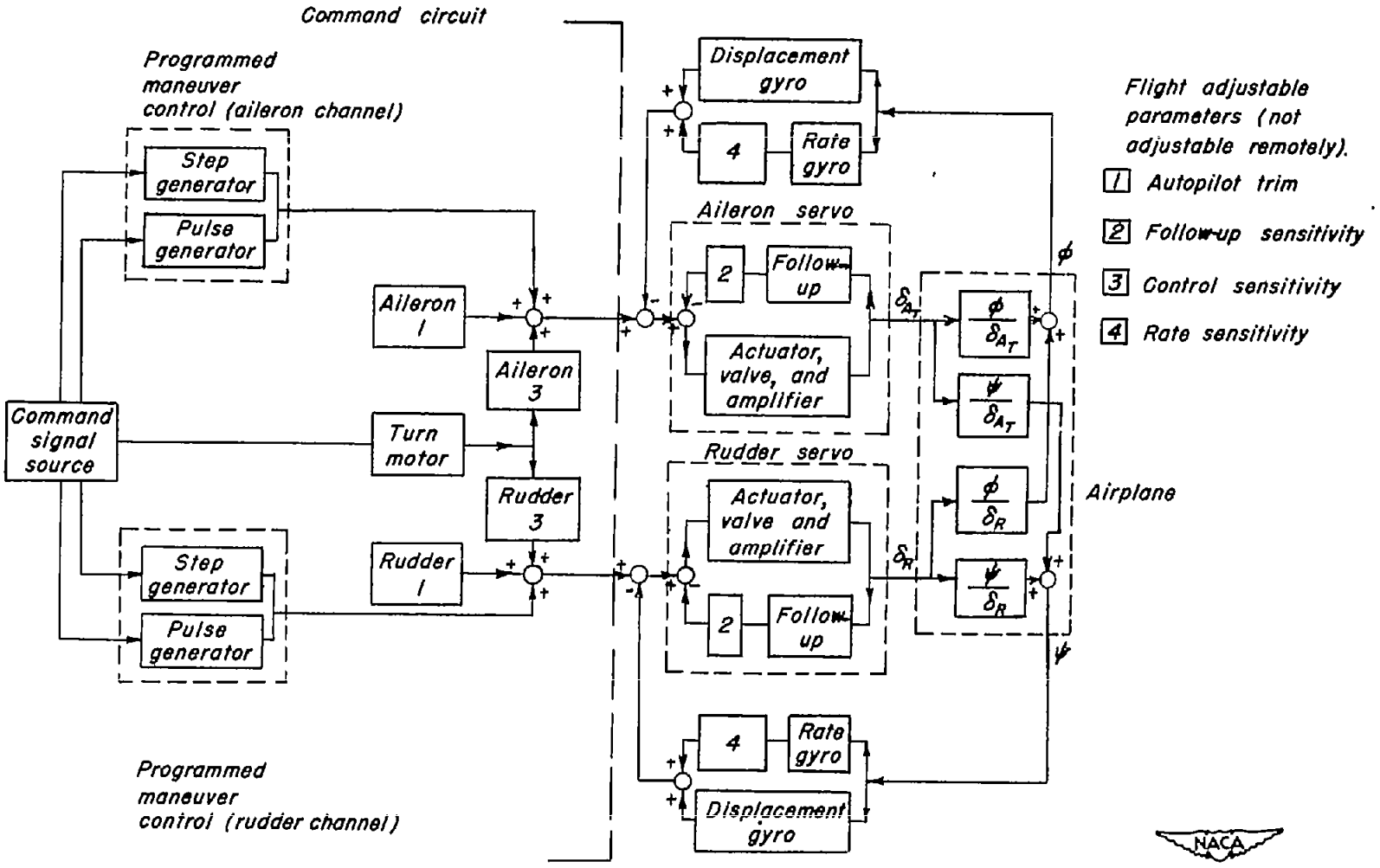

Figure 7.- Block diagram of the turn control channels, remote-controlled SB2C-5 drone #83135.

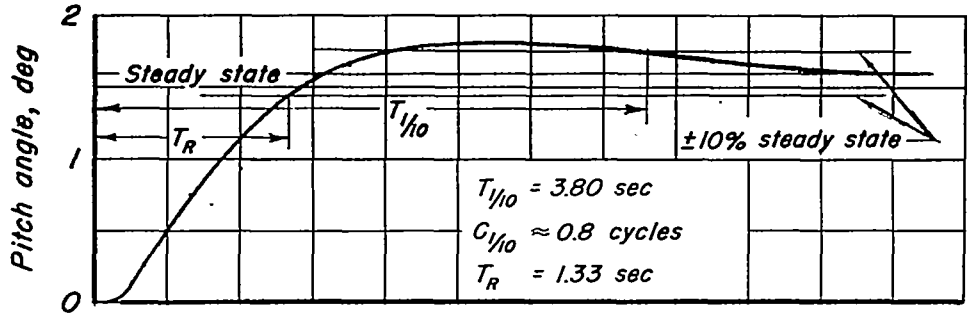

(a) Follow-up sensitivity 70.

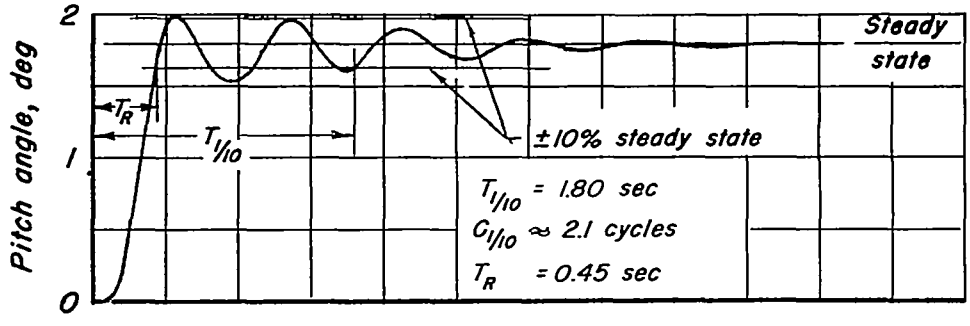

(b) Follow-up sensitivity 20.

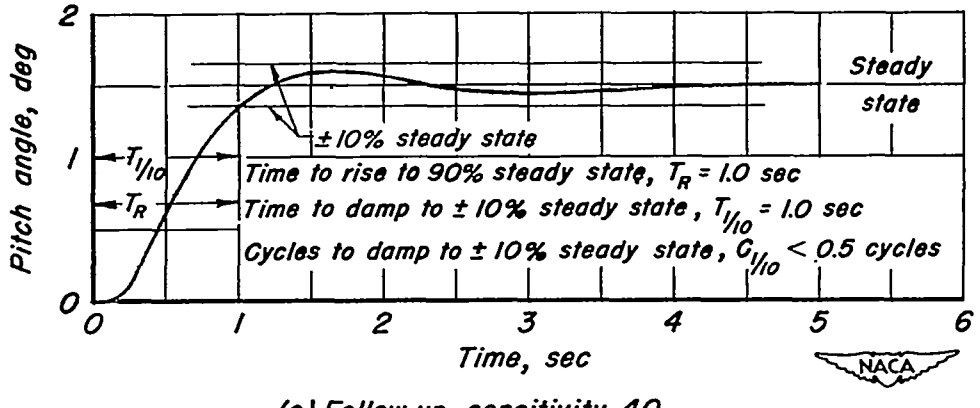

(c) Follow-up sensitivity 40.

Figure 8.- Effect of follow-up sensitivity on pitch response of airplane - autopilot combination, rate sensitivity 30, 130 knots, 10,000 feet.

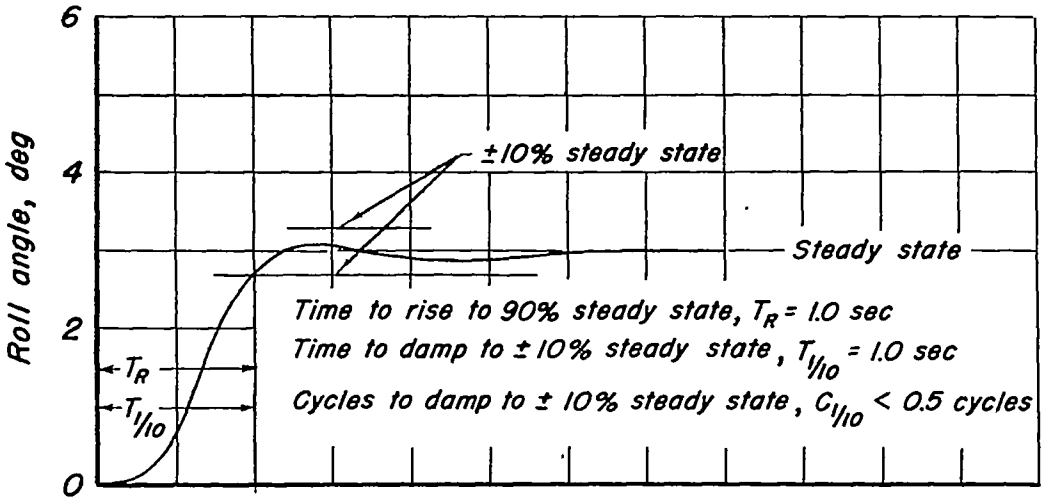

(a) Roll response to step input, rudder locked; follow-up sensitivity 45; rate sensitivity 30.

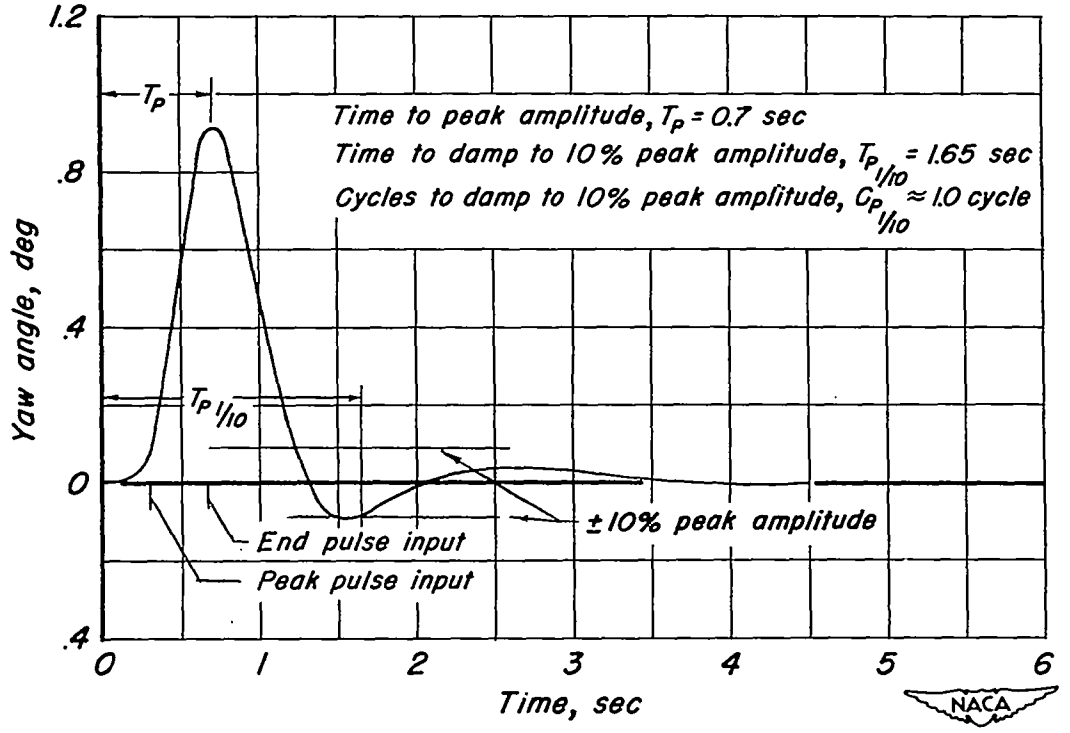

(b) Yaw response to a 2° pulse input, ailerons locked; follow-up sensitivity 50; rate sensitivity 40.

Figure 9.- Optimum lateral and directional transient-response characteristics of airplane - autopilot combination, 130 knots, 10,000 feet.

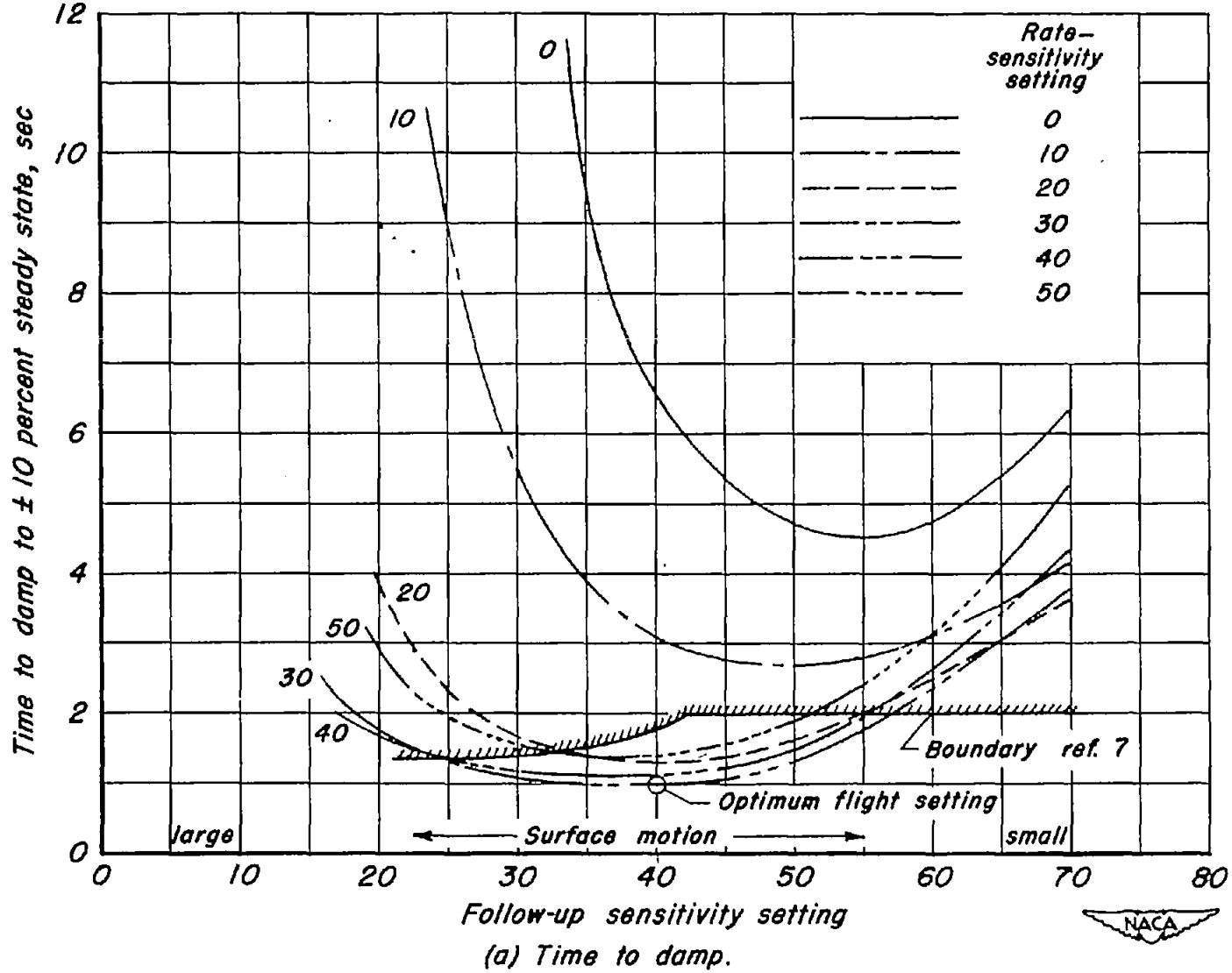

(a) Time to damp.

Figure 10.- Effect of parameter settings on the dynamic response of the airplane-autopilot combination due to a 2° step input in pitch, 130 knots, 10,000 feet, SB2C-5 drone #83135.

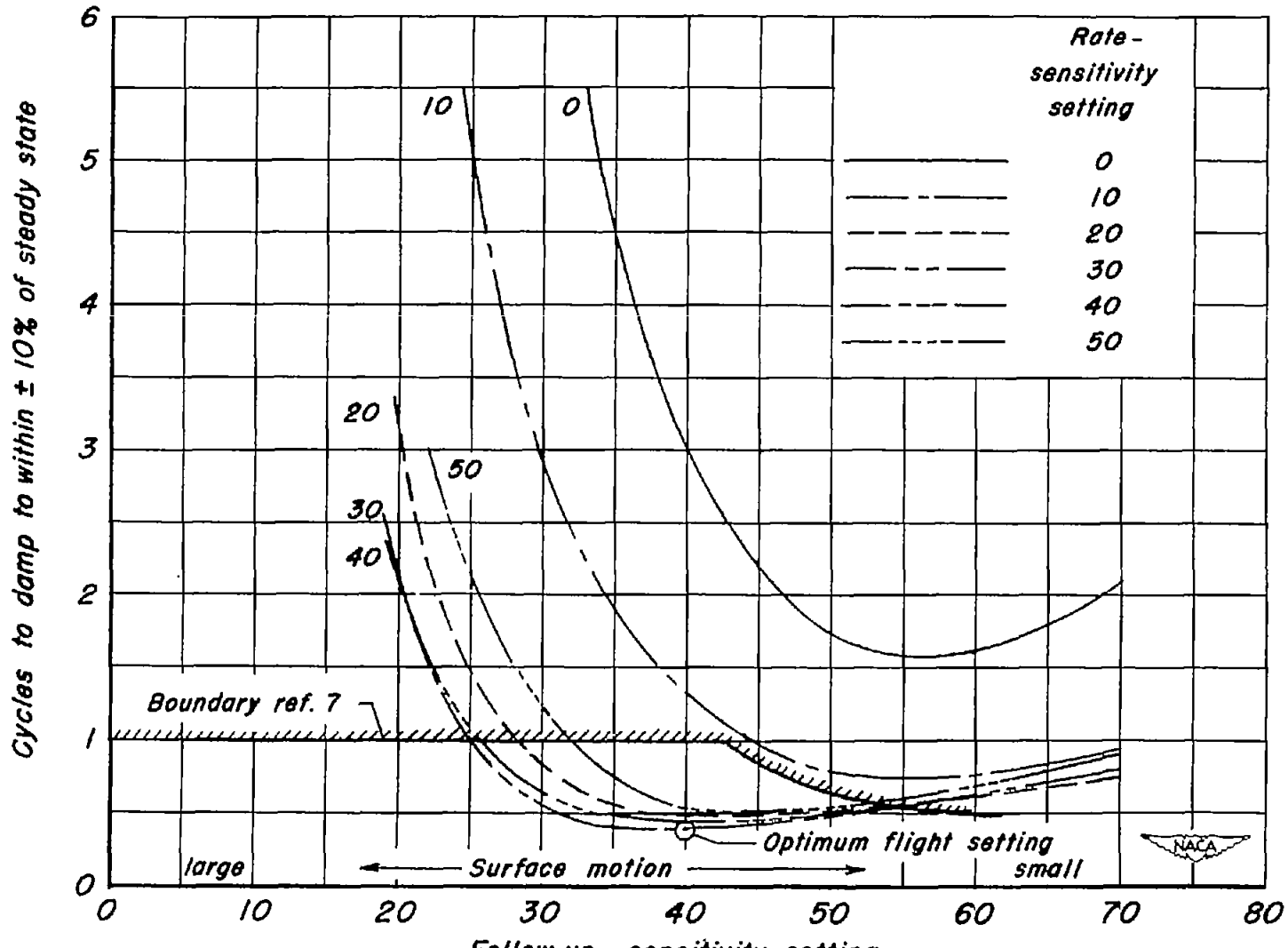

(b) Cycles to damp.

Figure 10.- Concluded.

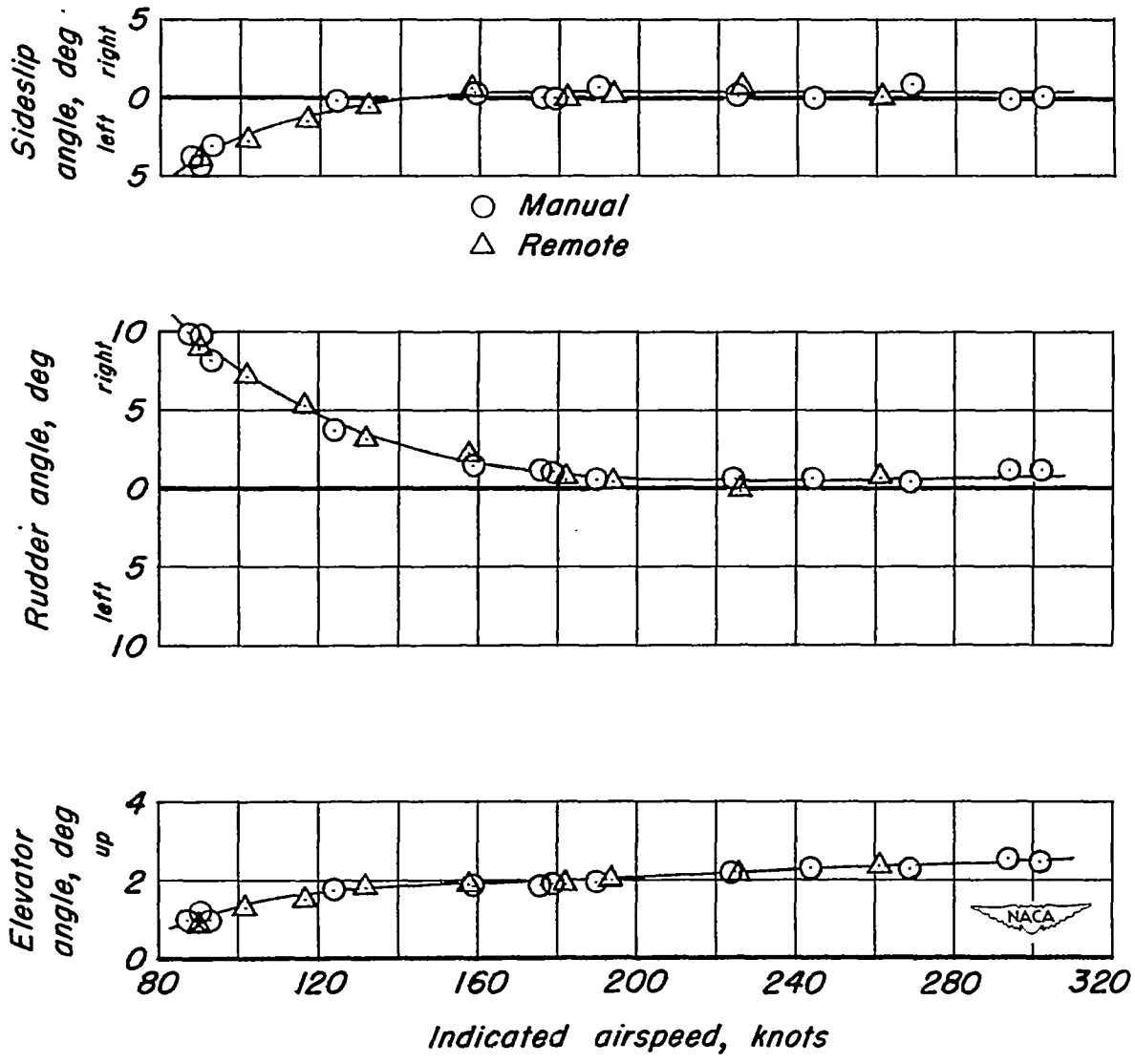

Figure 11.- Static longitudinal stability, normal rated power, flap and gear up, trim speed 180 knots, center of gravity 29.4% mean aerodynamic chord, 10,000 feet.

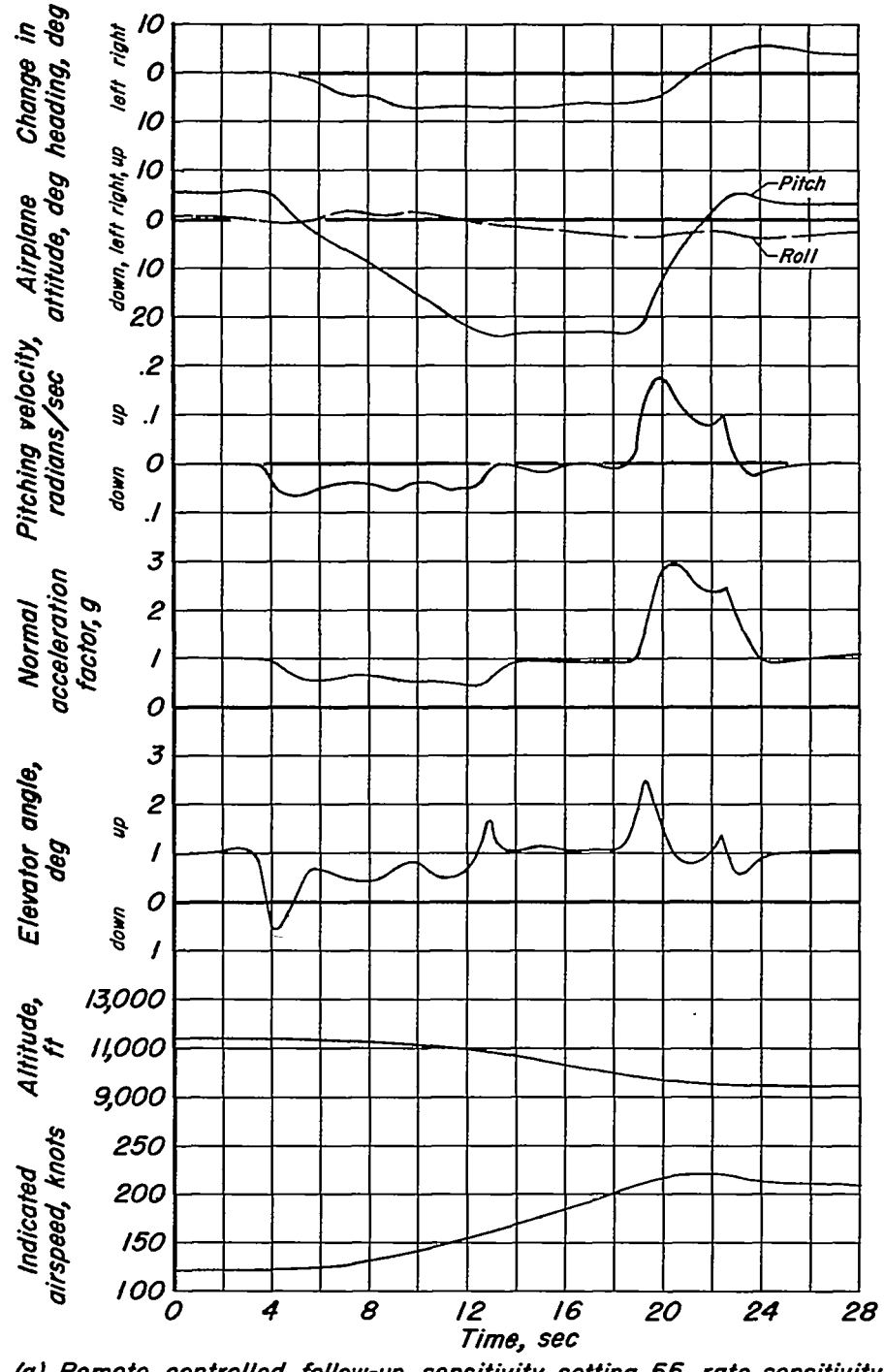

(a) Remote controlled, follow-up sensitivity setting 55, rate-sensitivity setting 30, dive-entry setting 3, dive-recovery setting 5.

Figure 12.- Time history of a dive entry, dive and dive recovery, SB2C-5 drone #83135.

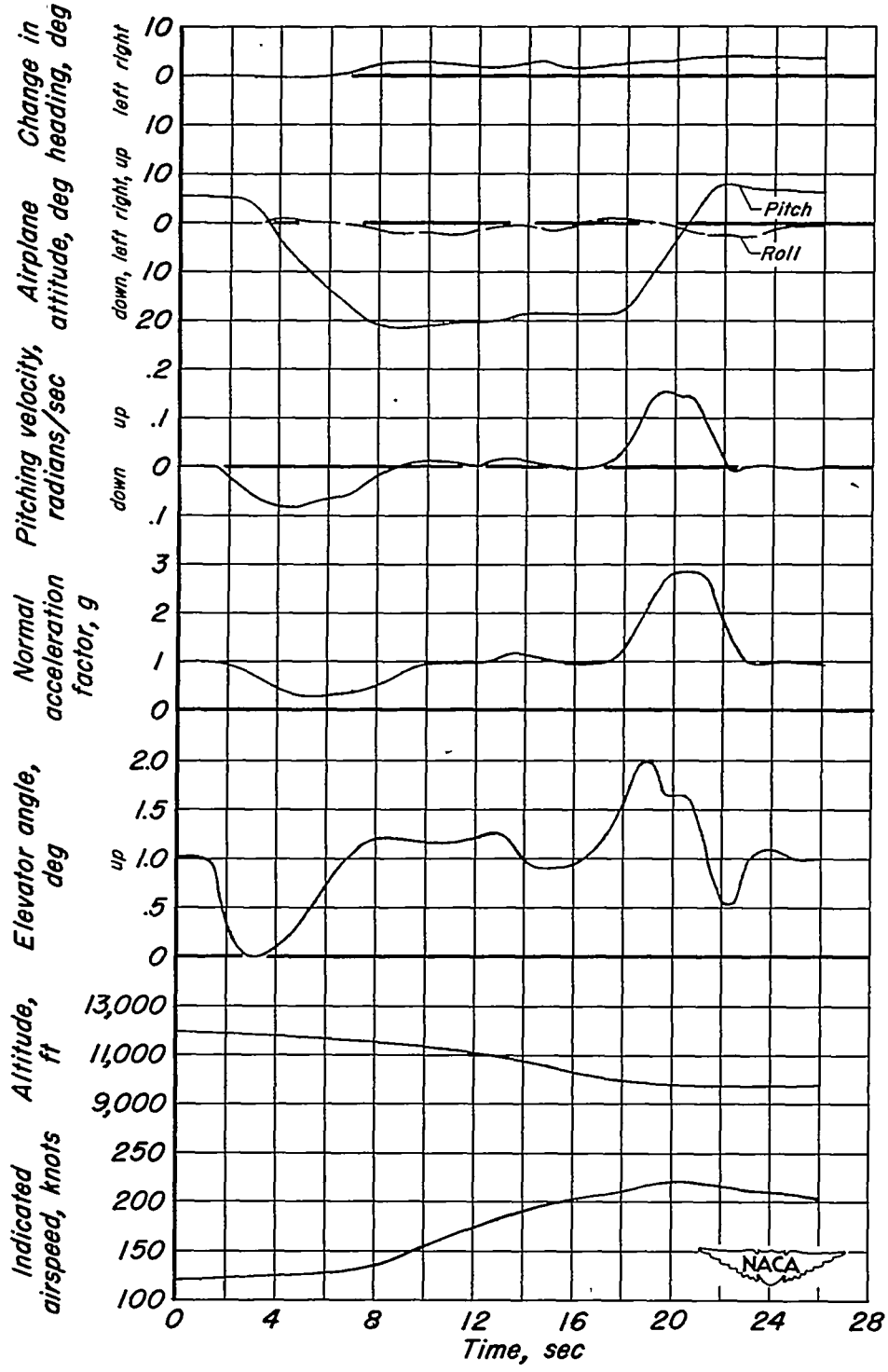

(b) Manually controlled.

Figure 12.- Concluded.

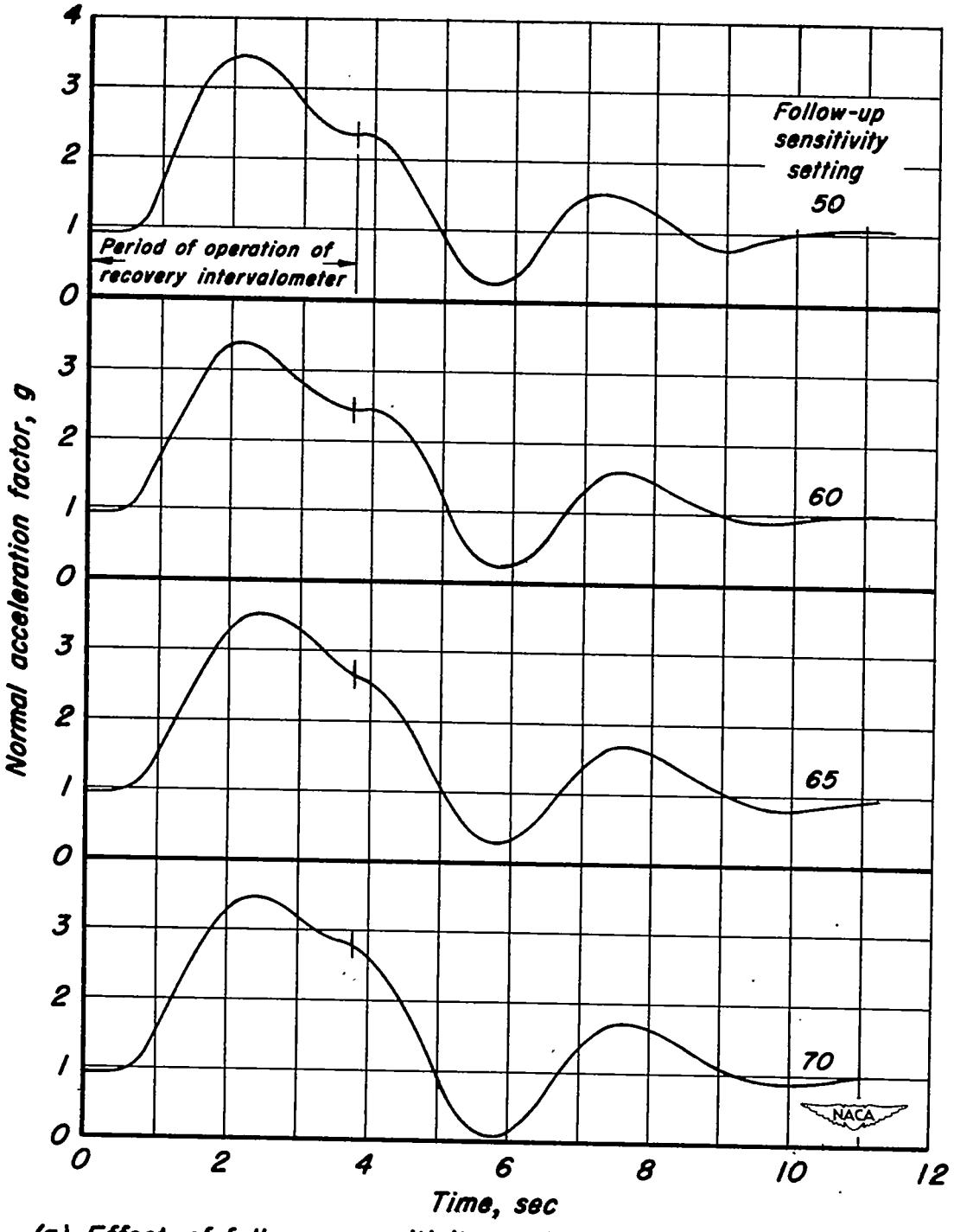

(a) Effect of follow-up sensitivity setting, dive-recovery setting 6.

Figure 13.- Effect of parameter settings on time history of a remote-controlled dive recovery. Rate-sensitivity setting 30, recovery airspeed 208 knots, dive angle -30°. SB2C-5 drone #83135.

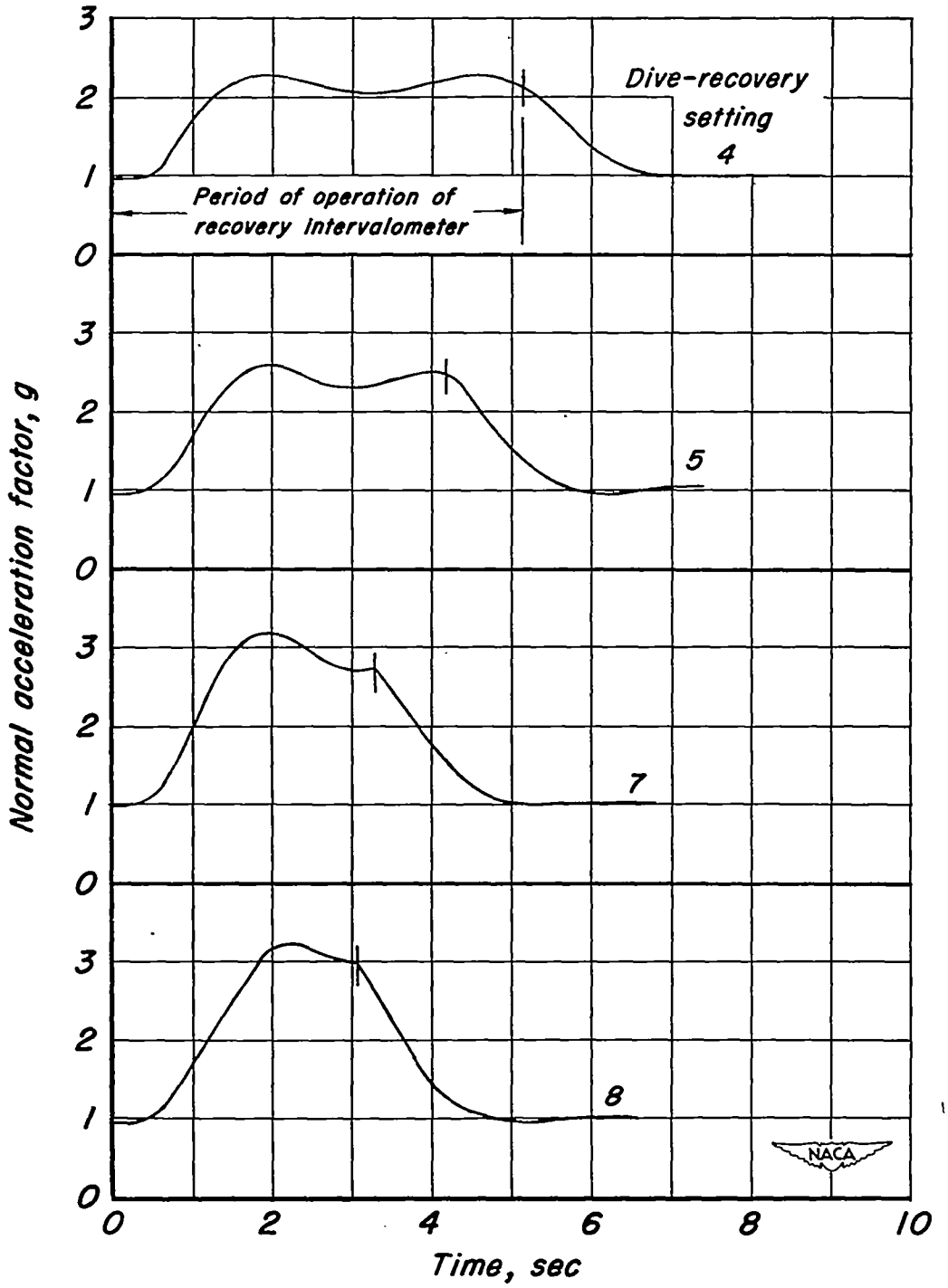

(b) Effect of dive-recovery setting, follow-up sensitivity setting 70.

Figure 13.- Concluded.

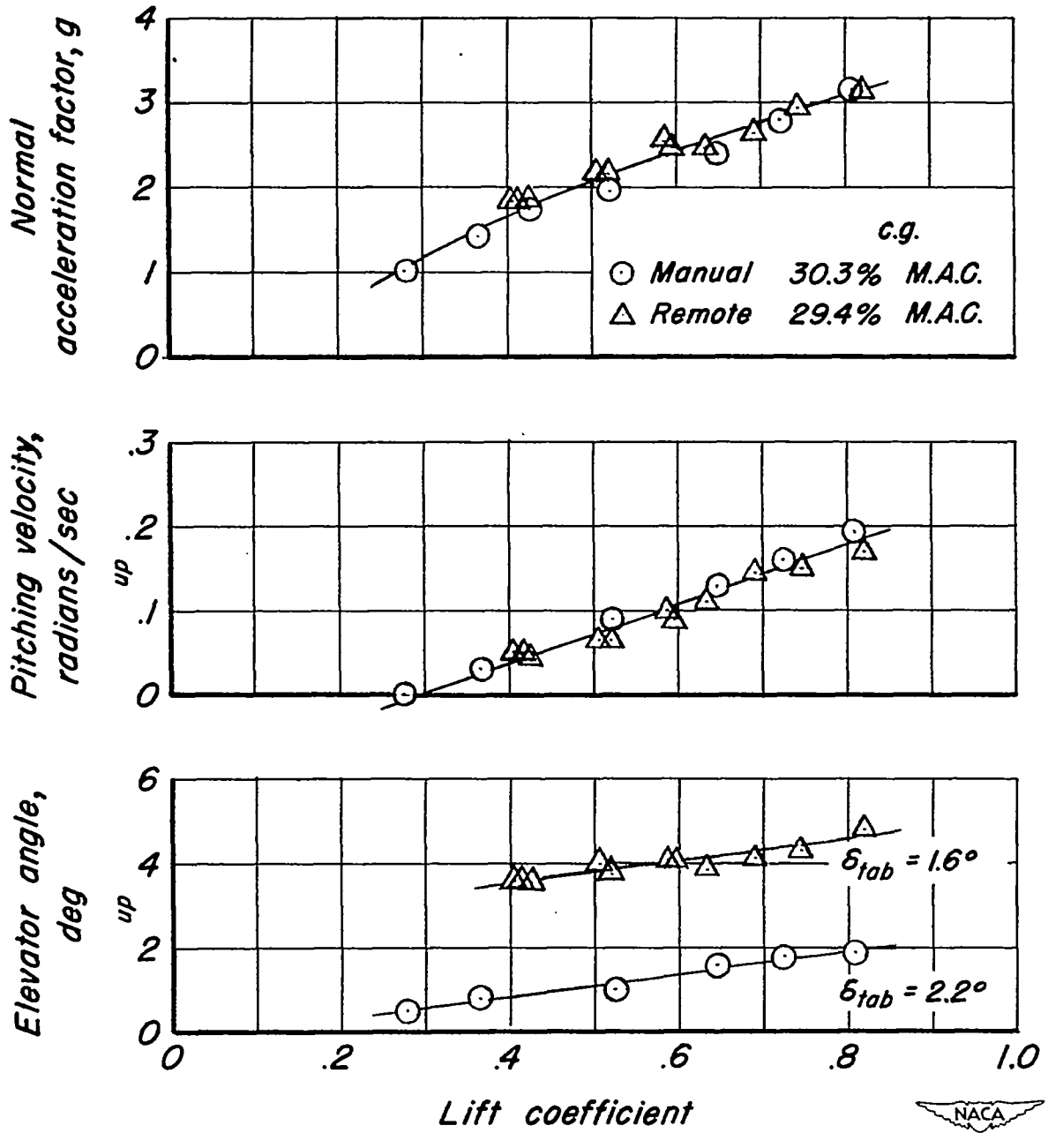

Figure 14.- Comparison of steady accelerated flight data produced under remote control and manual control, 180 knots, 10,000 feet, SB2C-5 drone #83135.

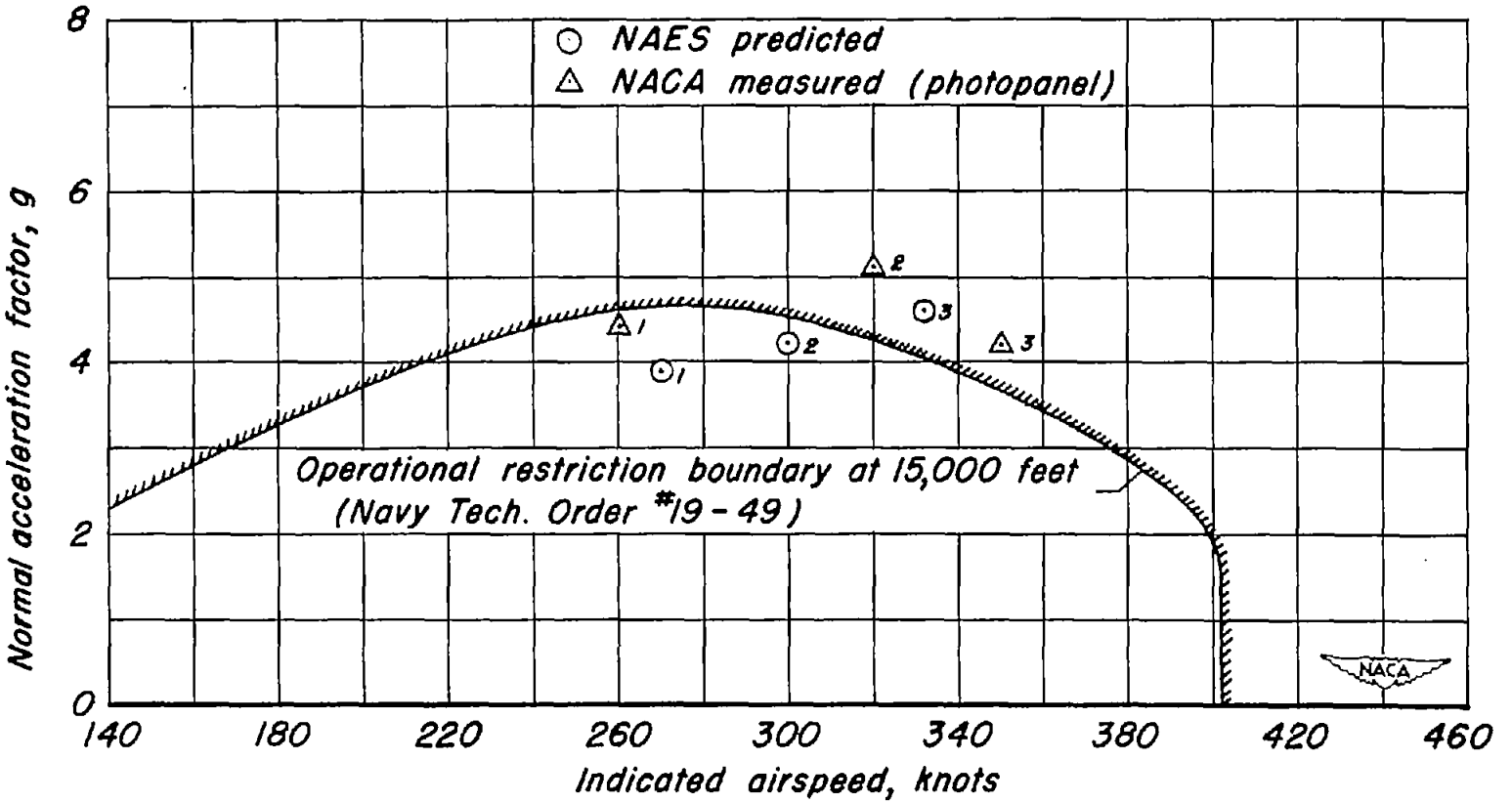

Figure 15.- Comparison between predicted and measured results of three dives of an F7F-3 drone operated nolo under radio remote control. Dive recoveries initiated at 15,000 feet by an altitude limit switch in the drone.

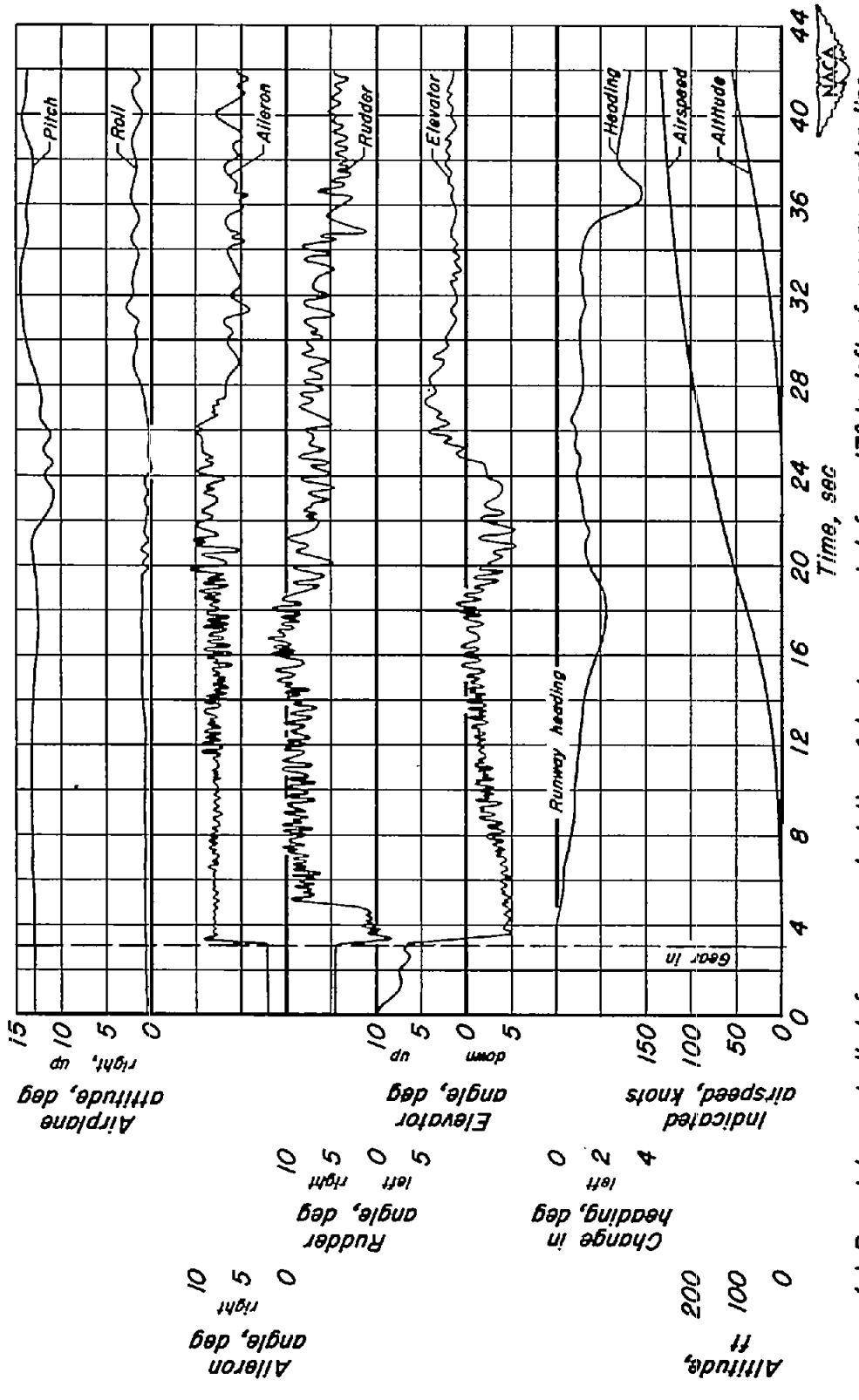

(a) Remotely controlled from ground station, 4 knot cross wind from 17° to left of runway center line. SB2C-5 drone #83135 with safety check pilot.

Figure 16.- Take-off time histories.

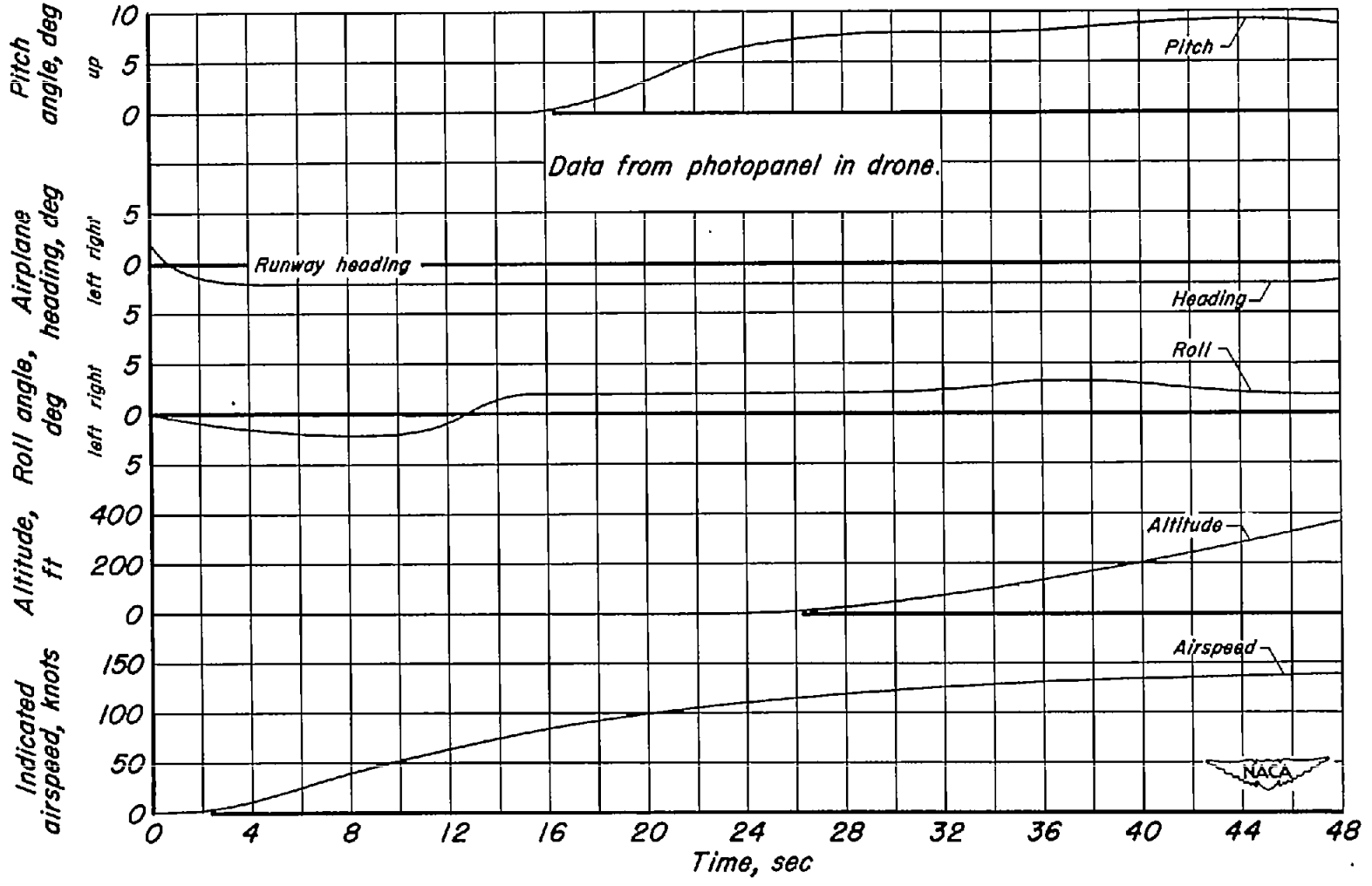

(b) Remotely controlled from ground station, 35 knot cross wind from 30° to left of runway center line, F7F-3 drone, nolo.

Figure 16.- Continued.

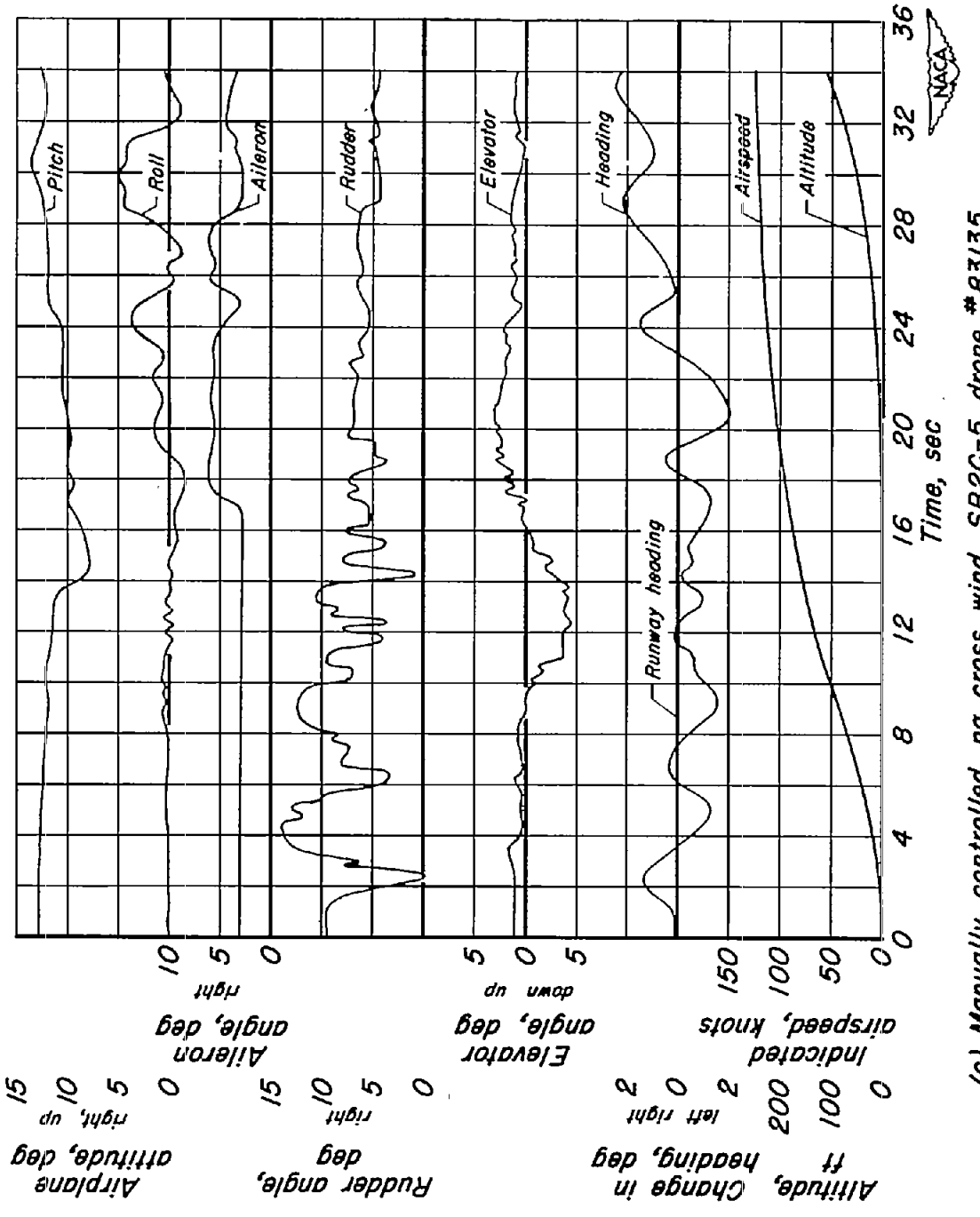

(c) Manually controlled, no cross wind, SB2C-5, drone #83135.

Figure 16.- Concluded.

(a) Remotely controlled from ground station, 4 knot cross wind from 17° to left of runway center line. SB2C-5 drone #83135 with safety check pilot.

Figure 17.- Landing time histories.

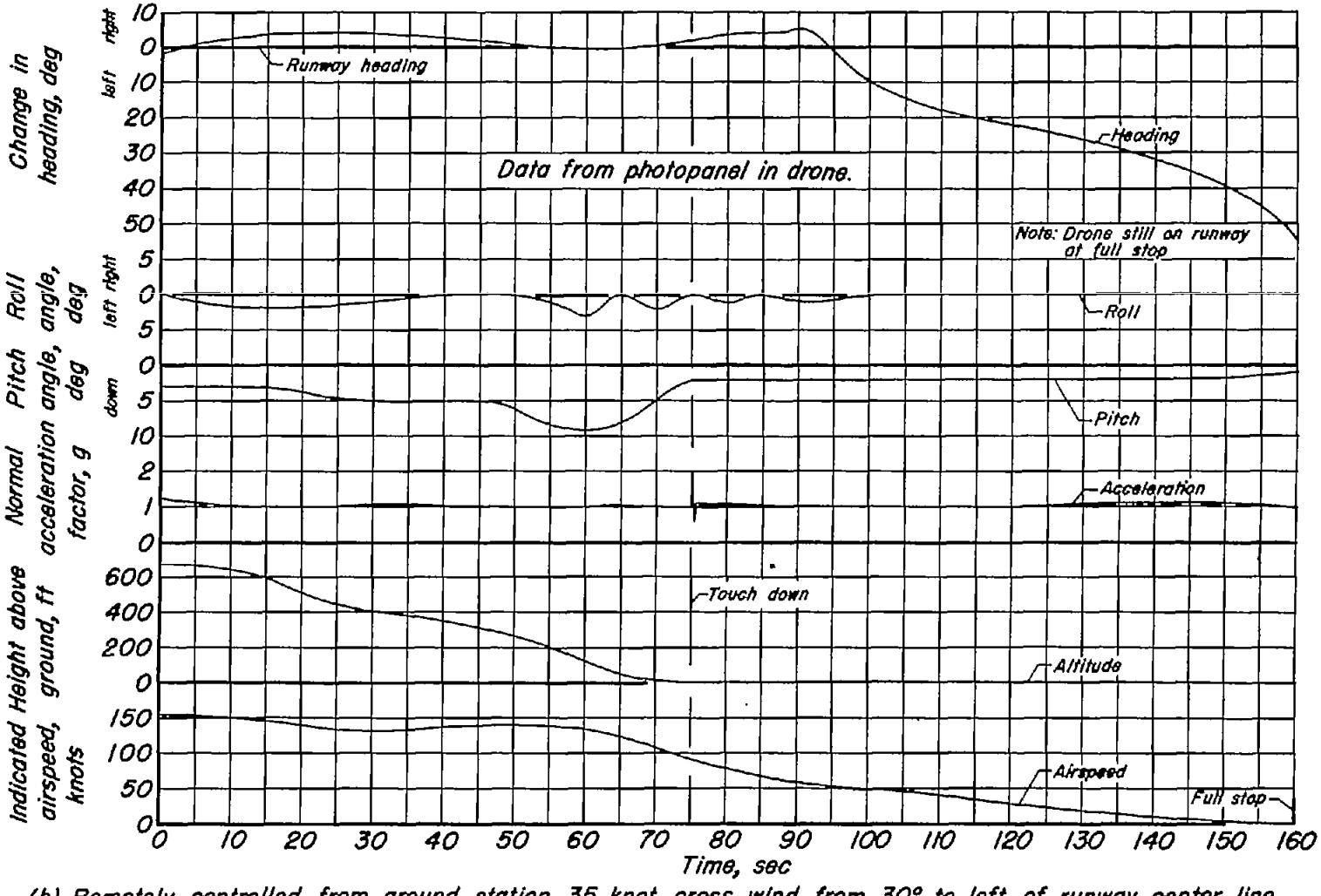

(b) Remotely controlled from ground station, 35 knot cross wind from 30° to left of runway center line, F7F-3 drone, nolo.

Figure 17.- Continued.

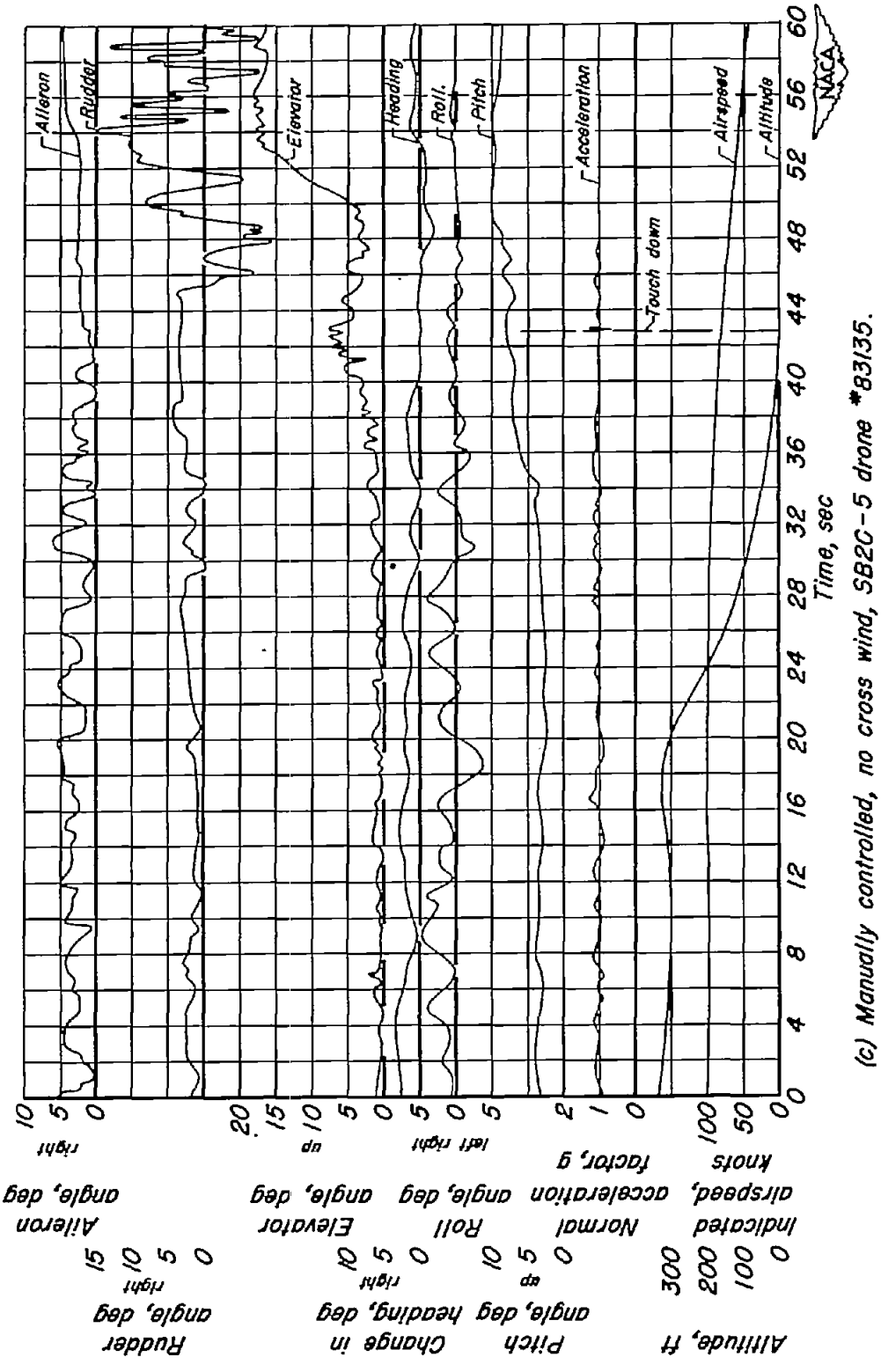

(c) Manually controlled, no cross wind, SB2C-5 drone *83135.

Figure 17.- Concluded.

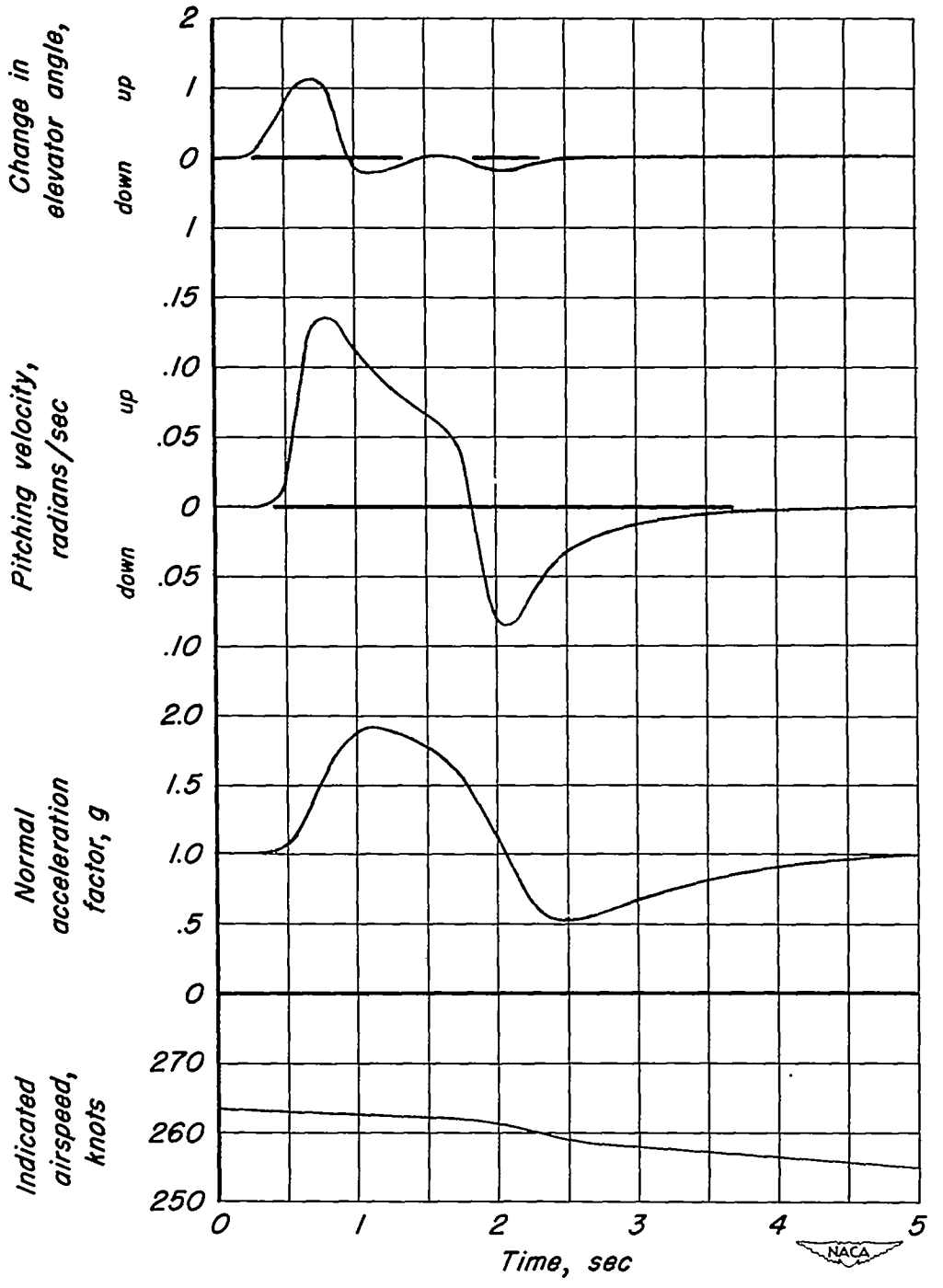

(a) Remote controlled, airplane destabilized in pitch.

Figure 18.- Time history of a longitudinal oscillation at 10,000 feet, SB2C-5 drone #83135.

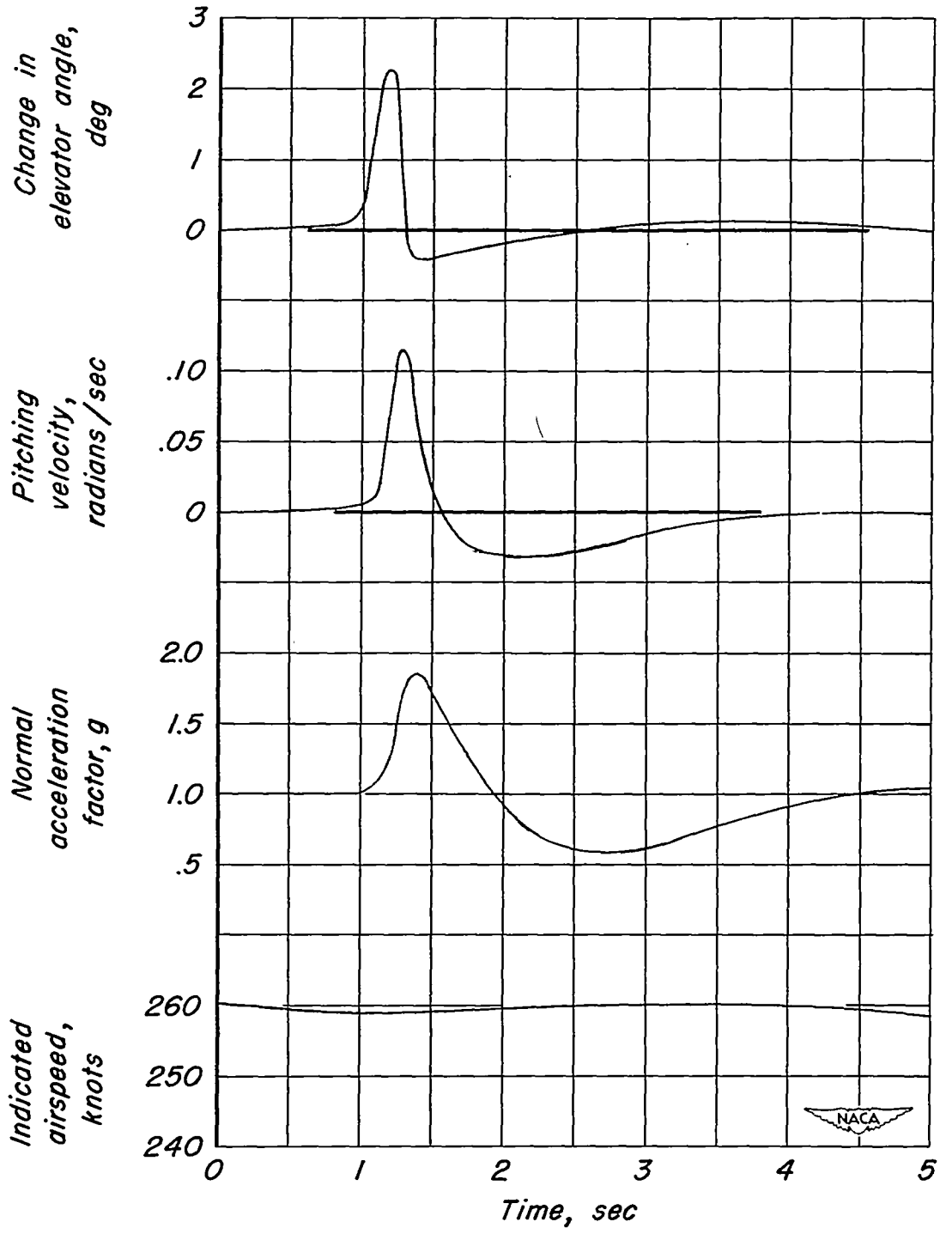

(b) Manually controlled .

Figure 18.- Concluded .

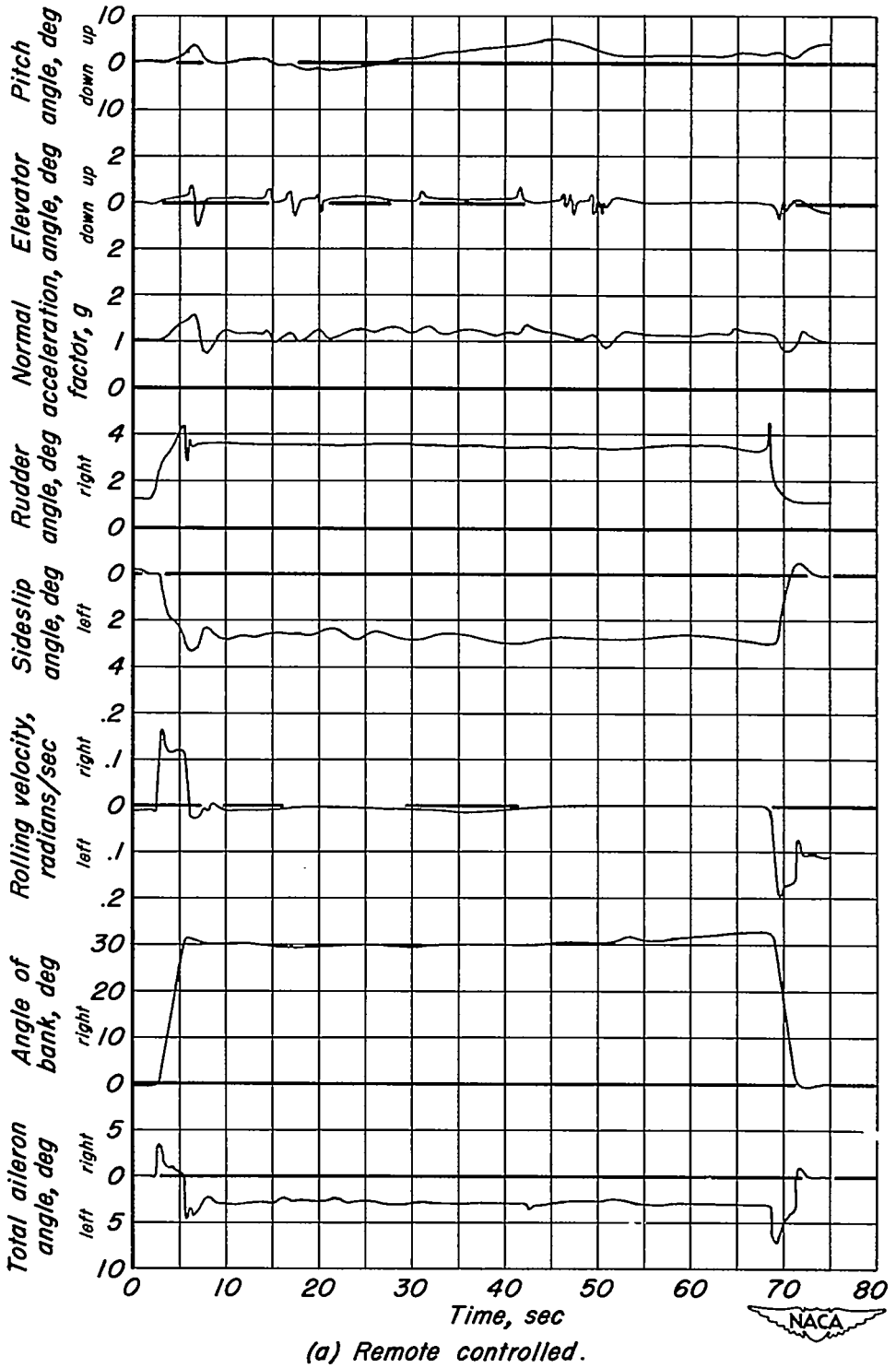

(a) Remote controlled.

Figure 19.- Time history of a 180° turn to the right, 190 knots, 10,000 feet, SB2C-5 drone #83135.

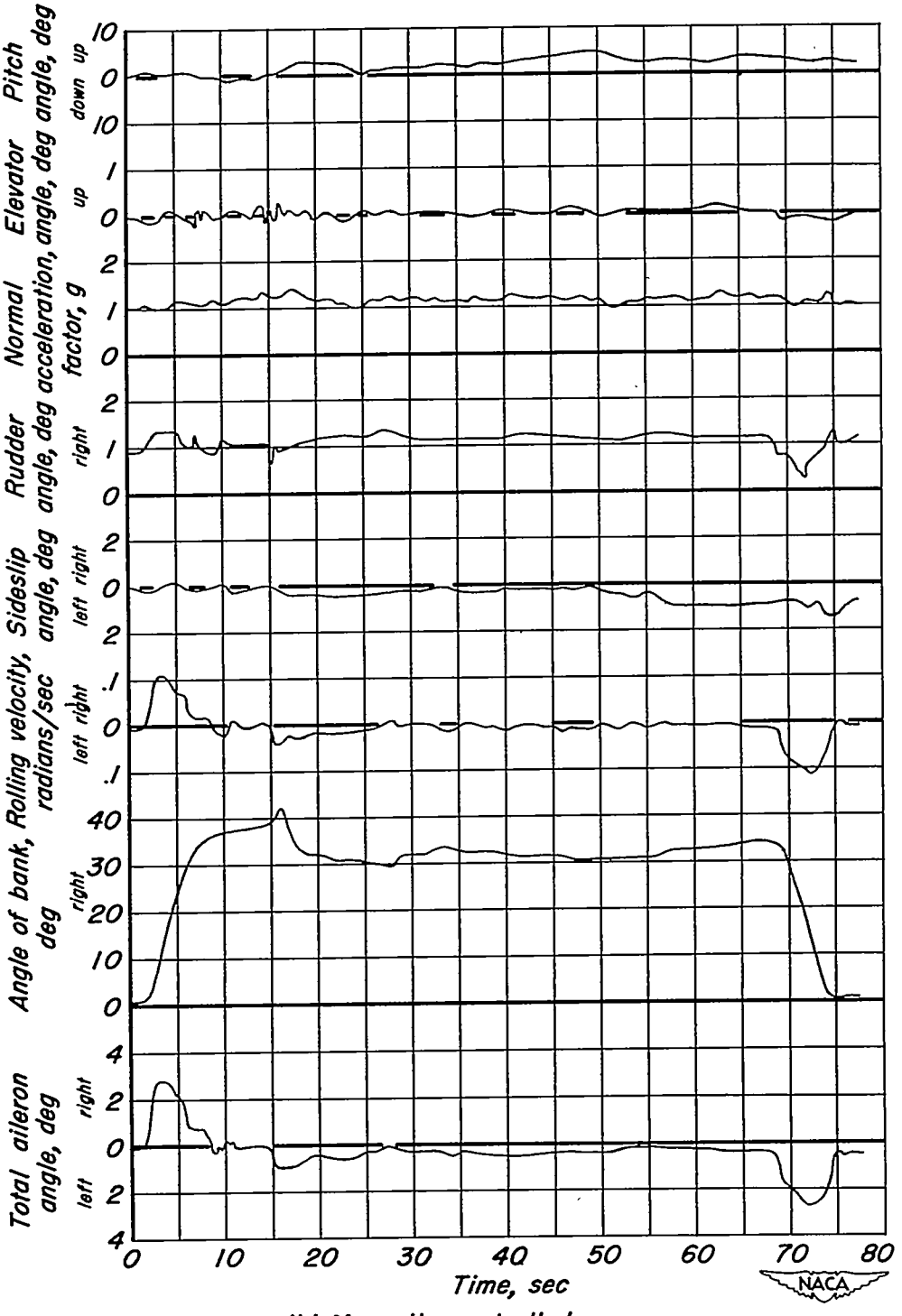

(b) Manually controlled.

Figure 19.–Concluded.

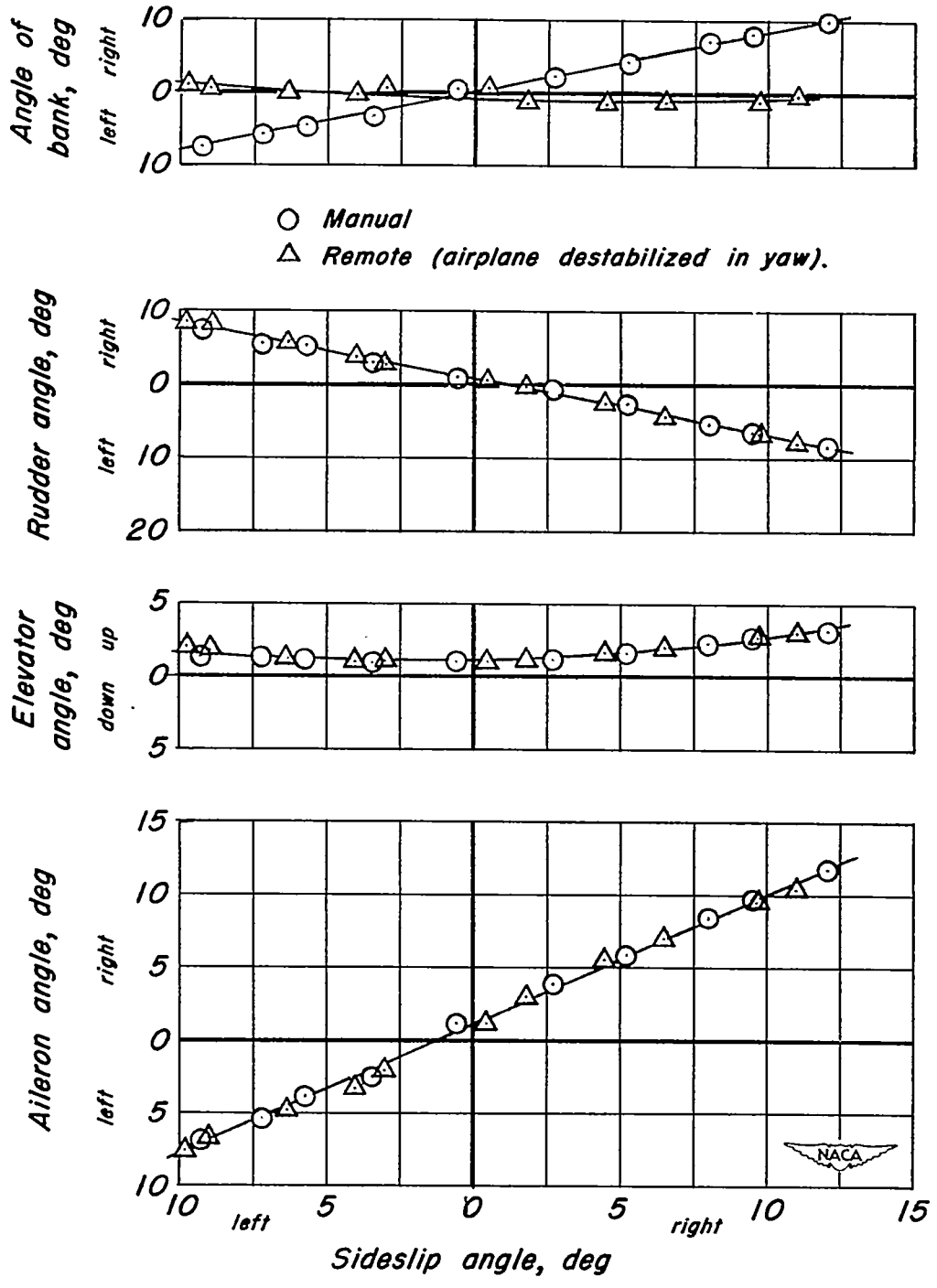

Figure 20.- Comparison of steady sideslips under remote control and under manual control, 130 knots, 10,000 feet, SB2C-5 drone #83135.

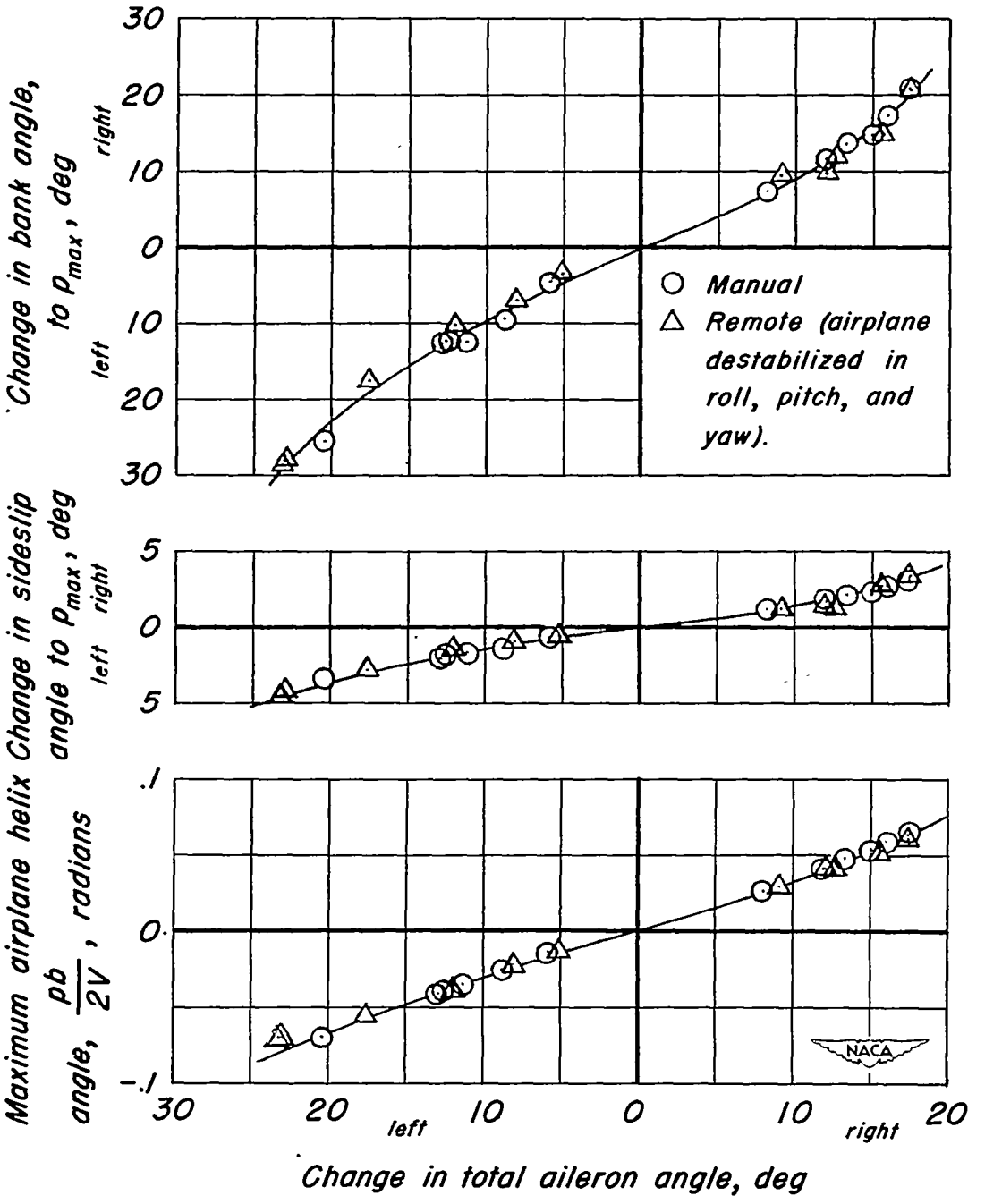

Figure 21.- Comparison between aileron rolls produced by remote control and by manual control, 130 knots, 10,000 feet, SB2C-5 drone #83135.

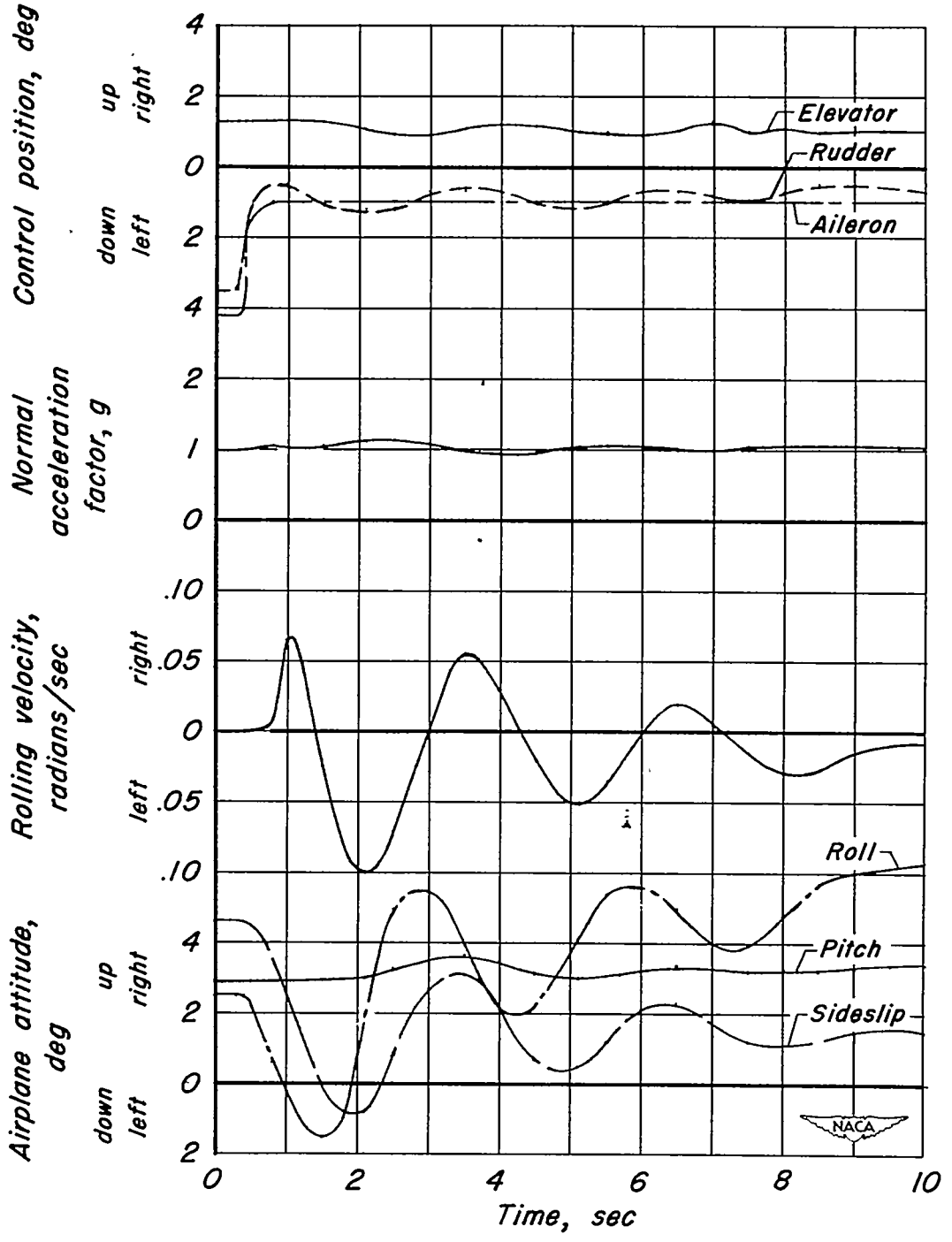

(a) Remote controlled, airplane destabilized in roll and yaw.

Figure 22.- Time history of a lateral oscillation from a steady sideslip, 182 knots, 10,000 feet, SB2C-5 drone #83135.

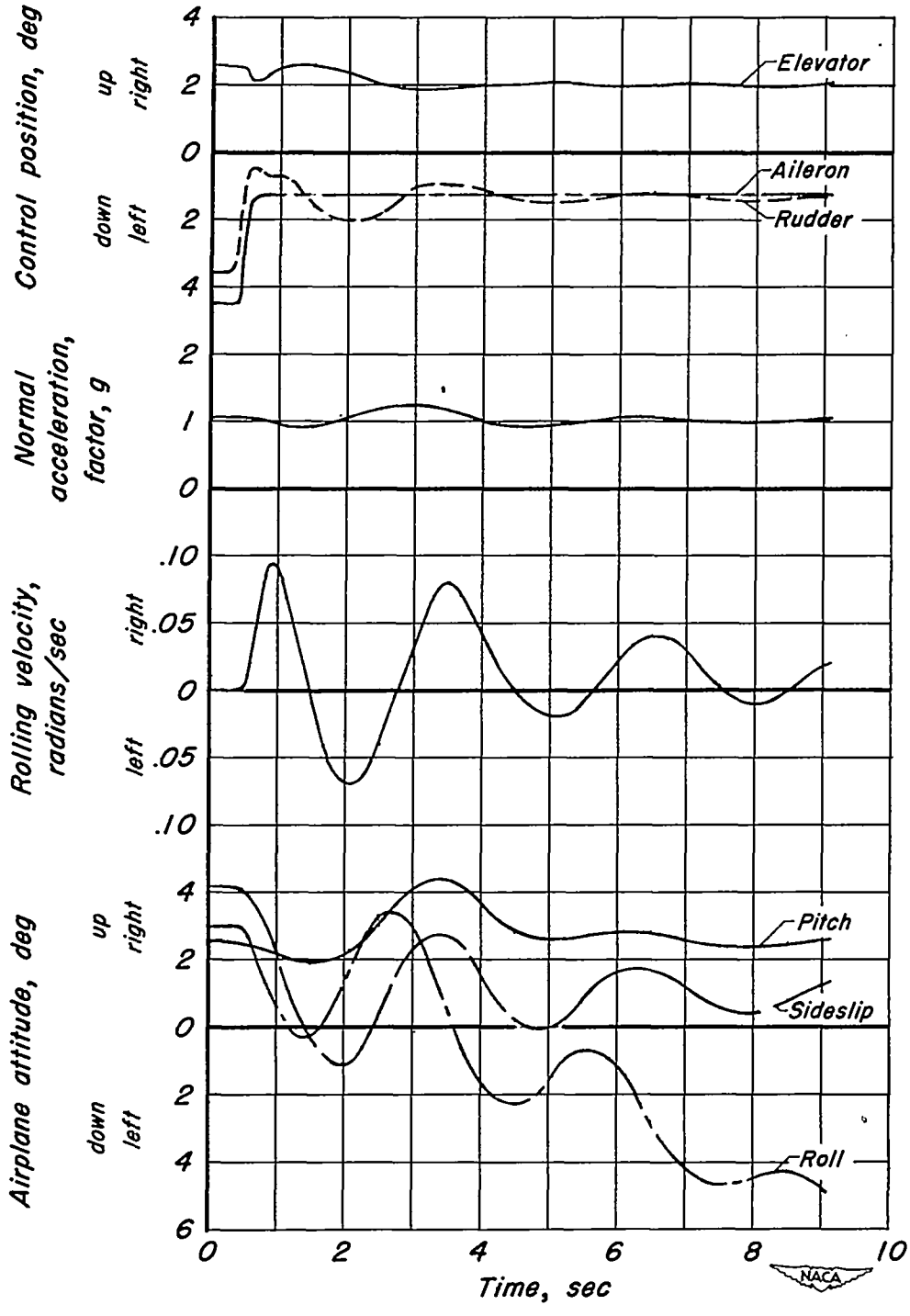

(b) Manually controlled.

Figure 22.- Concluded.

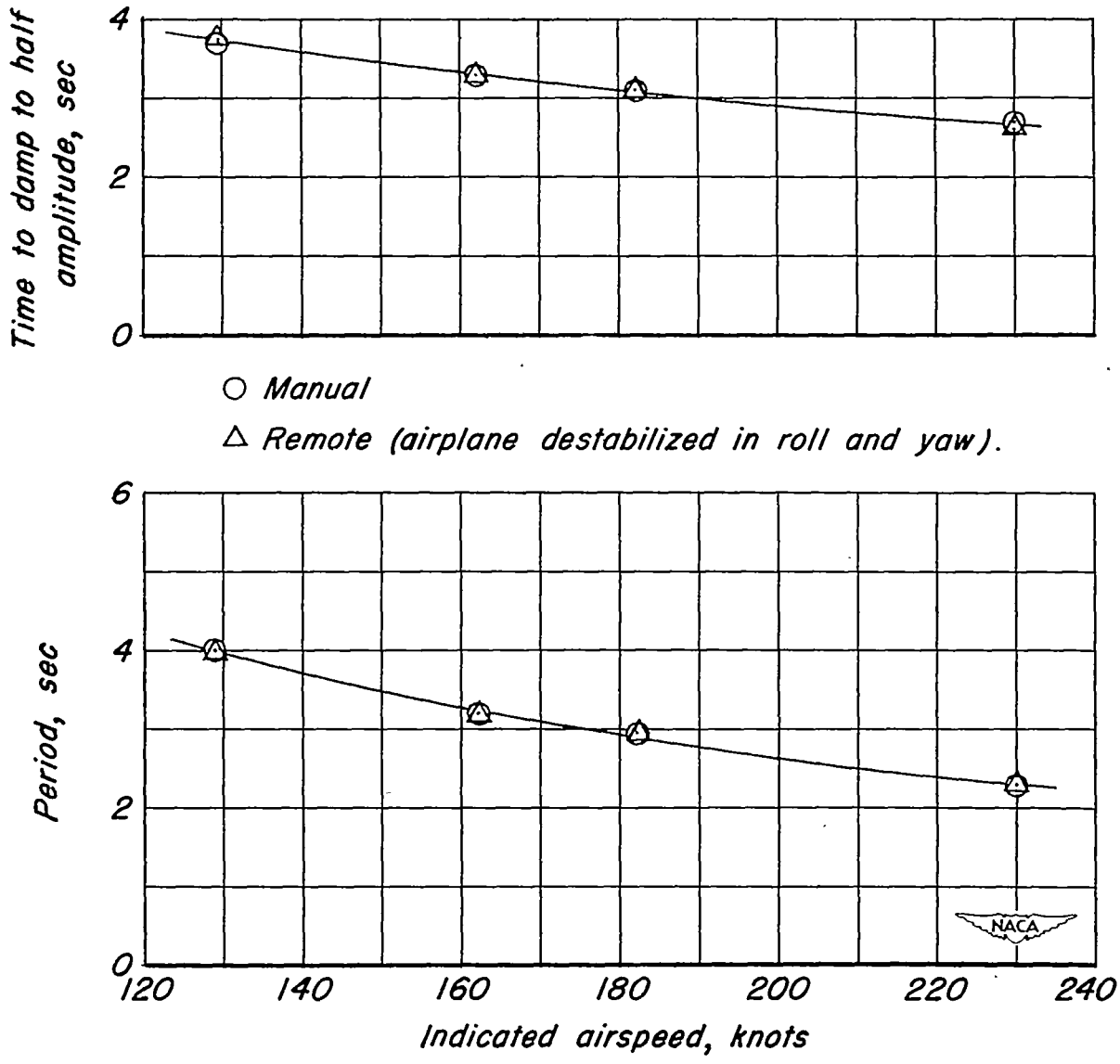

Figure 23.- Comparison of lateral oscillations produced from steady sideslips under remote control and under manual control, 10,000 feet, SB2C-5 drone #83135.

NACA-Langley - 3-29-55 -1000